8.0

Chapter 8 Lightwave based electrical noise measurements

Noise measurements form an important aspect when designing circuits and systems. Spectral measurements of equivalent input noise are valuable for specifying linear circuit performance, and the circuit designer may use them to improve the individual circuits before they are combined to a system. When required, the system designer may use these spectral measurements for predicting bit-error rates when these circuits are used in future systems.

Spectral noise measurements on electrical receivers, related to 50 Ω sources, are relatively simple when using calibrated electrical noise sources. This does not hold for *lightwave* receivers since lightwave noise sources are currently (1994) not commercially available.

This work resulted in novel methods for measuring the spectral noise of electrical amplifiers and lightwave receivers. In addition, these lightwave methods have significant advantages when applied to electrical noise measurements, compared to methods using conventional 50 Ω noise sources.

Spectral measurements, related to 50 Ω sources, are valuable for specifying circuit performance. Their value will vary with the circuit topology and the choice of device type and device biasing. As a result, spectral noise measurements, related to 50 Ω sources, are inadequate for specifying transistors and other circuit devices.

Spectral *noise parameters* of the individual devices are more suitable to predict the circuit noise for an arbitrary circuit topology. They are essential for reliable noise analysis in a simulator, and useful to improve the circuit design. Furthermore, measured noise parameters are crucial to develop new noise models of devices.

Synthesis of wideband noise-optimal amplifiers requires reliable noise models of transistors and other devices. Simple transistor noise models are commonly used [406] to successfully minimize noise at relatively low frequencies. When designing wideband lightwave receivers, we observed a disagreement between noise measurements and circuit noise analysis using these simple noise models. It requires a set of transistor noise parameters at various frequencies to develop improved noise models.

Manual methods for extracting device noise parameters using noise sources and impedance tuners are well-known and recommended since 1960 by IRE standards [818]. These measurements are quite laborious, and only recently some fully automated instruments have come to the market, mainly for microwave frequencies. As a result, complete sets of transistor noise parameters are sparingly specified, and if they are they are commonly restricted to a few distinct frequencies above 1 GHz.

This work resulted in novel methods for measuring two-port noise parameters, to facilitate future developments on improved transistor noise models. These methods are

8-2 8.5

an advantage when measuring below 1 GHz, compared to conventional methods using $50~\Omega$ noise sources cascaded by two-port impedance tuners.

This chapter describes various noise measurement methods on lightwave receivers, electrical amplifiers and transistors, using novel lightwave-based principles. It introduces new devices, calibration methods and measurement methods.

The measurement techniques proposed here rely on a novel lightwave device, a *synthetic noise generator*, providing white noise when illuminating PIN photo-diodes. This chapter is restricted to the application of this white noise source; the lightwave source is described in detail in chapter 9.

The highlights of this chapter, which are developed during the work on this thesis, are:

- Development of a new device, a *lightwave noise-tee* [802], applicable for calibration of synthetic noise, as well as generation of electrical noise. It is a multi-functional box, that has been used for various types of noise measurements.
- Development of a novel *multi-level noise source*, using a synthetic noise generator in combination with a lightwave noise-tee [802]. This combination has many advantages, in comparison to commonly used 50 Ω noise sources.
- Development of various *calibration* methods for synthetic noise, including attractive methods based on shot-noise calibration. The proposed shot-noise calibration is associated with high inherent accuracy (<1dB) obtained from simple dc-measurements. This is a significant advantage when initial calibration with primary noise standards is omitted.
- Development of new methods to *transform the calibration* of noise to arbitrary reference planes, using mathematical halving of noise-tees. The transformation method facilitates noise measurements using arbitrary source impedances.
- Development of a novel method to measure equivalent input noise of *lightwave receivers* [801, 803: patent pending]. This method facilitates noise measurements valid at the *optical* input of the receiver (usually the receiver noise is specified at an internal electrical reference plane behind the photo detector).
- Development of a novel algorithm to extract *equivalent input noise* of an optical or electrical device under test. It facilitates *multi-level* noise measurements to improve the measurement accuracy of noise measurements at comparative measurement time. This means that more reference levels are used than the commonly used 'hot' and 'cold' noise levels. The multi-level noise source is matched to the transmission line that links the source with the device under test.
- Development of a novel algorithm that *generalizes* the two-port *noise parameter* extraction of an electrical device under test, with known input impedance. The algorithm holds for any combination of noise sources, each with arbitrary effective 'temperature' and impedance. When more then five different sources are used, the algorithm extracts the most plausible solution, by minimizing the *relative* error. The algorithm includes the application of *multi-level* noise measurements.

This chapter is restricted to spectral density measurements on noise. Other measurements, such as BER measurements, are not considered. Furthermore, correction for out of band effects, such as spurious response errors, are not discussed.

8.1. The art of measuring noise

Noise measurements can be performed as *direct* noise measurement as well as *ratio* noise measurement. Both methods results in *absolute* noise figures, although ratio-noise measurements are superior in accuracy and simplicity. Typical aspects of both methods are listed below:

- For *direct* measurements the output noise spectrum of an amplifier under test is measured with a calibrated selective voltmeter, such as a spectrum analyzer or a noise figure meter. Another type of measurement determines the gain of the amplifier. The input noise is reconstructed from the measured output noise by division by the measured gain. The source and load impedances of the measurement are kept equal to the source and load impedance of the application.
- For *ratio* measurements, a calibrated white noise source is connected to the input of an amplifier under test. The *relative* change in output noise spectrum is measured when the level of the calibrated noise source is varied (usually switched between 'high' and 'low'). The input noise is reconstructed from this relative change and from the known noise levels of the noise source. The *absolute* value of the amplifier output spectrum is irrelevant.

This section discusses both measurement methods, to illustrate the superiority of ratio noise measurements. They are the most convenient, because the measurement accuracy is mainly determined by the calibration accuracy of a (simple) noise source. The remainder of this chapter is mainly restricted to ratio measurements.

8.1.1. Pitfalls while measuring noise

High accuracy is hard to obtain for direct methods. Spectrum analyzers are convenient instruments for this purpose, however ± 2 dB amplitude uncertainties are common values. This accuracy holds for detection for harmonic signals and not for noisy signals. The accuracy is reduced for noise by built-in envelope detectors, logarithmic amplifiers and fast sweeping filters with variable resolution bandwidth. This can be explained as follows [804]:

- The built-in detector is usually not a true-rms detector, but is based on a much simpler top detector. When its detection level is calibrated for Gaussian distributed noise, it provides erroneous results when the statistic distribution of the input signal is non-Gaussian (we observed 0.2 dB difference when using our synthetic noise source, as described in section 9.2.4).
- The built-in logarithmic amplifier modifies the statistic distribution which prevents correct noise detection, even when an rms-detector is used [804]. This effect can be eliminated when the spectrum analyzer is used in true linear mode.
- Variation of the resolution bandwidth varies the detected noise level, while this level will not vary when detecting harmonic signals.

As a result, when a spectrum analyzer is used in log mode, and noise corrections are restricted to resolution bandwidth correction, the average noise is displayed approximately 2~2.5 dB *too low*! [804]

Ratio measurements are insensitive to scaling errors in the frequency selective voltage detection. Gain and resolution bandwidth measurements are not required, and mis-match errors will hardly decrease the overall accuracy. Therefore, the accuracy of ratio

measurements is mainly restricted to the accuracy of the calibrated noise source. Since this device is simple, it is easy to calibrate it with high accuracy; ± 0.1 dB are common values. As a result, ratio noise measurements are superior in accuracy and simplicity, compared to direct noise measurements

8.1.2. Accuracy limits when measuring noise

An increasing number of spectrum analyzers is equipped with (hidden) calibrated noise marker facilities, to simplify their use in direct noise measurements. These facilities perform the required error corrections automatically, and create the impression of accuracy. This is because the measurement accuracy for noisy signals with unknown statistic distribution is always lower than the accuracy for harmonic signals. These limitations are more significant when logarithmic receivers are used then when linear receivers are used. This is discussed below and in section 9.2.4.

Accuracy limits in logarithmic receivers (as in many spectrum analyzers)
 The spectrum analyzer is primarily intended for detecting signal components of which the spectral width is small compared to the resolution bandwidth. An additional noise marker corrects for systematic errors [804], and its calibration is commonly based on natural (Gaussian distributed) noise.

To simplify matters a noise marker calibration is assumed with equal accuracy performance as applies to harmonic signals. The noise marker calibration corrects for errors originating from the use of an envelope detector, to simulate an rms detector. When the statistic distribution of noisy signals differs from Gaussian distributions then this correction will fail. This yields an additional uncertainty, which makes the overall accuracy for noise detection lower than for harmonic signal detection

Furthermore, replacement of the envelope detector by a true-rms detector will not always resolve this problem with the noise marker accuracy. A logarithmic amplifier compresses the peaks of noisy signals and modifies their statistic distribution before it is detected. As a result, the combination of true-rms detection with logarithmic amplification remains sensitive to variations in statistic distribution.

• Accuracy limits in linear receivers (as in many noise figure meters)

To improve the measurement accuracy for noisy signals, commonly used noise figure meters (e.g. HP8970a) are implemented as linear receiver¹, in stead of logarithmic receivers. This makes them more dedicated to noise measurements but slower responding on large signal variations.

Although these instruments are dedicated to noise measurements, it is not a matter of course that they are equipped with *true-rms* detection (HP8970a uses an envelope detector). This increases the overall measurement uncertainty, compared to true-rms detection, when non-Gaussian distributed signals are detected.

A remaining noise accuracy problem arises from the spectral width of noisy signals. Frequency selective receivers are sensitive to out-of-band signals (spurious

¹ These instruments are equipped with switched attenuators to scale the input signal within the linear detection range of the noise detector. Since this requires an iterative adjustment when the signal level changes, these linear receivers are slower responding then receivers with logarithmic converters.

response). This results from inter-modulation by non-linear distortion and from insufficient image rejection. The wider the spectral width is, the more signal is erroneous detected. This inaccuracy increases with the magnitude of the noisy signal. As a result, spectral noise detection suffers from additional accuracy reduction, compared to spectral detection of harmonic signals.

The use of additional filtering (preselection), before heterodyne mixing, will improve the accuracy, however this is commonly not a standard feature in spectrum analyzers.

In general, ratio noise measurements are less sensitive to the above mentioned accuracy limits. This holds especially when the statistical distribution, spectral width and spectral level of the calibrated noise source equals the noise of the device under test.

8.1.3. Basic definitions

In ratio noise measurements, the output noise power of the device under test varies with the noise level of the calibrated noise source. It is often convenient to relate these noise levels to thermal noise. The terms cold noise, excess-noise and hot noise are defined as follows:

- Cold noise is the output noise of the device under test, when the noise source is switched 'off'. The lowest noise level of this source equals the thermal noise of its source impedance at room temperature, for instance R=50 Ω and T=290 K. The intensity spectrum of this noise level will be referred as $S_c(\omega)$.
- Excess noise is what an activated noise source adds to the cold noise level. This level will be referred as $S_e(\omega)$.
- Hot noise is the output noise of the device under test when the noise source is switched 'on'. It is the combination of cold-noise and excess-noise. Since they are uncorrelated, the intensity spectrum of this noise is $S_h(\omega) = S_c(\omega) + S_e(\omega)$.

An important figure of merit of calibrated noise sources is the ratio of their excess noise level and cold noise level. The *excess noise ratio* (in dB) of a noise source is defined as: $ENR_dB = 10 \cdot log(S_c/S_c) = 10 \cdot log(S_h/S_c-1)$.

Level S_h is the (hot) spectral intensity when the source is switched on, and S_c the (cold) spectral intensity when the source is switched off.

When the ENR of a source are specified and the cold noise level is a known reference level, the associated excess noise and hot noise levels can be extracted from these values. The cold noise level is usually the thermal noise of the source impedance, at the IRE *standard reference temperature*. according to IRE standards [817], this temperature is defined as T=290K This is rather cold for convenient room temperature, however, it has been chosen because (kT/q)=0.0250V (q=elementary charge).

Room temperature is usually 2% higher, and for that reason automated noise figure meters such as an HP8970a use T=296.5K as default reference temperature.

8.2. Multi-level noise source with lightwave noise-tee

In order to carry out ratio noise measurements on electrical amplifiers, various white noise sources are commercially available. Most of these sources are provided with fixed output impedance (50Ω) and with fixed on and off noise levels.

The use of more than two calibrated noise levels is attractive to reduce random measurement errors by redundancy. The use of output impedances other than 50Ω is attractive when measuring noise levels below the thermal noise level of 50Ω resistors.

This study has resulted in the introduction [802] of a new lightwave device, called a *noise-tee*², for generating white electrical noise. It uses a lightwave synthetic noise generator [901,902,907], also resulted from this study. The noise-tee has attractive additional features, compared to commonly used 50Ω noise sources, including:

- Noise level in 'off'-state is significantly lower than thermal noise of 50Ω resistors.
- Noise level is variable over a wide dynamic range (ENR: 0-40dB, ore more).
- Relative accuracy of noise level is based on simple transfer measurements.
- Absolute accuracy of noise level is based on simple calibration at low frequencies
- Scaling accuracy of noise level is based on simple dc current measurements.
- Output impedance is variable over a wide dynamic range (up to $100 \text{ k}\Omega/(0.2\text{pF})$).
- Output impedance is insensitive to variation of noise level.
- Applicable in one-port and two-port configurations.

This subsection describes the proposed noise-tee and its performance.

8.2.1. Circuit diagram of a noise-tee

Figure 8.1 shows the basic circuit diagram of the noise-tee [802]. The noise-tee is a transmission line (e.g. microstrip or stripline), that is shunted in the middle by an illuminated PIN photo-diode. White noise is generated in this diode using a lightwave *synthetic noise generator* [901,902,907], a new lightwave device that is described in chapter 9. The PIN photo-diode is (externally) biased, and the dc photo current through the PIN photo-diode is (externally) sensed to detect the illumination power.

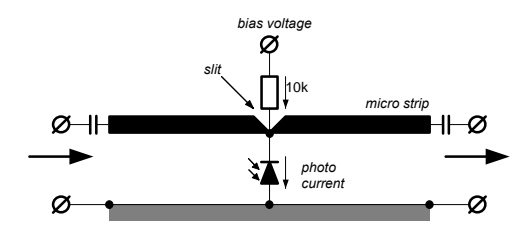


Fig 8.1 Basic circuit diagram of a lightwave noise-tee. A noise current is generated in a photo-diode that is shunted to a (microstrip) transmission line. The microstrip slit compensates for the diode capacitance.

(200) Lightwave based electrical noise measurements

R.F.M. van den Brink

² The name (lightwave) *noise-tee* is proposed in [802], and inspired to the name 'bias-tee'. A noise-tee injects a noise current in a transmission line while a bias-tee injects a dc-bias current.

As a matter of course, a simple one-port construction with a PIN photo-diode, shunted by a 50Ω resistor, is adequate to implement a 50Ω noise source. This situation is similar to our two-port configuration of figure 8.1, with an external 50Ω resistor on one of its ports. Nevertheless, the symmetrical two-port construction increases the flexibility of the device, as will be demonstrated in this chapter. It enables an external modification of source impedance.

The high impedance of the photo-diode causes a minimal degradation of the propagation performance of the transmission line. The most annoying effect is the parasitic capacitance of the PIN photo-diode. Nevertheless, capacitance values below 0.2pF are feasible with naked chips. A microstrip slit (see figure 8.1) is effective in compensating these parasitic capacitances.

All noise-tee experiments in this chapter are based on a 50Ω microstrip construction on 1.5 mm glass-epoxy board, 4 cm long, and based on a 1 pF photo-diode with 2.5 nH serial inductance. The overall responsivity of this construction is flat up to 1.5 GHz.

8.2.2. Variable noise source based on a matched noise-tee configuration

One of the noise-tee applications is its usage in a stand-alone *electrical* noise source. Figure 8.2 shows the associated (matched) configuration. The lightwave output signal of a synthetic noise generator is fed to the noise-tee using a variable optical attenuator and an optical fiber. The illumination generates a white noise current in the PIN photodiode, proportional with the illuminated optical power. The photo current is externally measured with an pico-ampere meter to detect this illumination power.

The left side of the noise-tee is externally matched to the characteristic impedance Z_0 of the internal transmission line of the noise-tee (see figure 8.1). As a result, the output impedance at the right side becomes Z_0 too, e.g. Z_0 =50 Ω . Furthermore, it prevents the output level of the source from being frequency dependent when the internal noise-tee transmission lines have non-zero lengths.

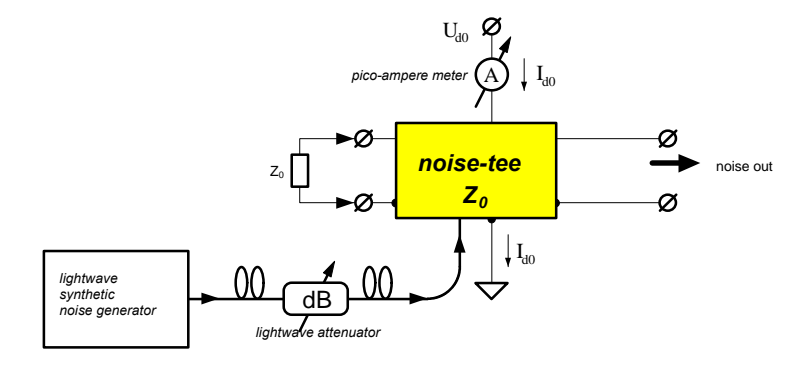


Fig 8.2 Matched noise-tee configuration to implement an electrical noise source with variable output level. The ratio between photo current I_{d0} and spectral current density (\mathring{OS}_{ie}) of the excess-noise is insensitive to optical power variations.

Lightwave synthetic noise generators (see chapter 9) may generate noise that is white over several hundreds of gigahertz [902]. The magnitude of the noise-tee frequency response, from optical input port to electrical output port, is independent of the transmission line length when both sides are loaded with Z_0 . As a result, the lightwave frequency response of the noise-tee is mainly limited by the bandwidth of the PIN photo-diode. A bandwidth of more than 10 GHz is feasible.

The lightwave frequency response of the noise-tee can be measured simply and accurately with a heterodyne setup. Therefore, it is adequate to calibrate the noise current in a small frequency band, and use the lightwave frequency response to extrapolate this value to other frequencies. In many applications, this extrapolation is simple because PIN photo-diodes have a flat frequency response over a wide frequency interval.

8.2.3. Output noise level of a matched noise-tee configuration

One of the most attractive features of a matched noise-tee configuration (figure 8.2) is that the output noise level is continuously variable, when using an optical attenuator. Since the minimum output noise level is restricted by the thermal noise of the internal and external resistors, it is convenient to relate the various noise contributions to thermal noise. Usually, the terms cold noise, excess-noise and hot noise apply, as defined in section 8.1.

- Cold noise is the output noise of the configuration in figure 8.2, without illumination. The intensity spectrum of this current will be referred as $S_{ic}(\omega)$.
- *Excess-noise* is the synthetic noise current flowing through the photo-diode. The intensity spectrum of this current will be referred as $S_{ia}(\omega)$.
- Hot noise is the total output noise of an illuminated noise-tee: The intensity spectrum of this current is $S_{ih}(\omega) = S_{ic}(\omega) + S_{ie}(\omega)$.

The cold noise mainly originates in the external (50 Ω) load (in figure 8.2 on the left side of the noise-tee). When this load is removed, the cold noise is significantly reduced, and is limited by the thermal noise originating from the internal bias resistors (e.g. $10k\Omega$, or higher). When this external load is cooled, the cold noise level reduces, without affecting the output impedance and excess-noise level. This might be an advantage for dedicated microwave measurements on (cooled) ultra low-noise amplifiers.

The excess-noise originates from the illumination by the lightwave synthetic noise generator. The amplitude spectrum of this current ($\sqrt{S_{ie}}$) is proportional to the illuminating power.

The responsivity of the PIN photo-diode is independent of the optical power, which means that the *ratio* between dc photo current (I_{d0}) and the spectral current density ($\sqrt{S_{ie}}$) of the excess-noise is a constant over a wide dynamic range. We verified this experimentally in reference [802].

This property is of great value when the excess-noise level is varied with an optical attenuator. Once calibrated at a specific reference noise level S_{ie0} , the excess-noise of the setup in figure 8.2 is accurately scaled to an arbitrary noise level $S_{ieX} = (I_{dX}/I_{d0})^2 \cdot S_{ie0}$ when the dc photo current I_d is measured with a simple (pico)-ampere meter.

The maximum excess-noise of a noise-tee configuration is significantly higher than for calibrated noise sources such as an HP346c (50Ω , ENR=13dB, 10MHz to 26GHz). This is because synthetic noise generation is a power efficient process (section 9.2.3).

For example, assume a lightwave synthetic noise generator that provides synthetic noise over B=50GHz bandwidth using a 1mW laser at 1300nm. Under these circumstances, the mean (dc) photo current in the noise-tee is roughly I_{d0} =0.5 mA. Using the theory on synthetic noise generation, as discussed in section 9.2.3 and 9.3.2, the calculated excessnoise current density is approximately $\sqrt{S_{ie}}\approx1.6$ nA/ \sqrt{Hz} . This value is more that 87 times higher than the thermal noise current in a 50 Ω resistor $\sqrt{S_{ie}}\approx18$ pA/ \sqrt{Hz} , which demonstrates the high excess-noise level that is available (ENR ≈39 dB).

8.2.4. Output impedance variation of a noise-tee configuration

Another attractive feature of a matched noise-tee configuration (figure 8.2) is that the output impedance is insensitive to variations of the output noise level, over a wide dynamic range. Figure 8.3 demonstrates this in competition with an HP346c noise source.

The change in output impedance is negligible for the proposed noise-tee, while an HP346c noise source is liable to $\pm 10\%$ impedance variations when it is switched between on and off. This impedance variation may result in measurement errors when the noise contribution and the gain of an amplifier under test vary with the source impedance.

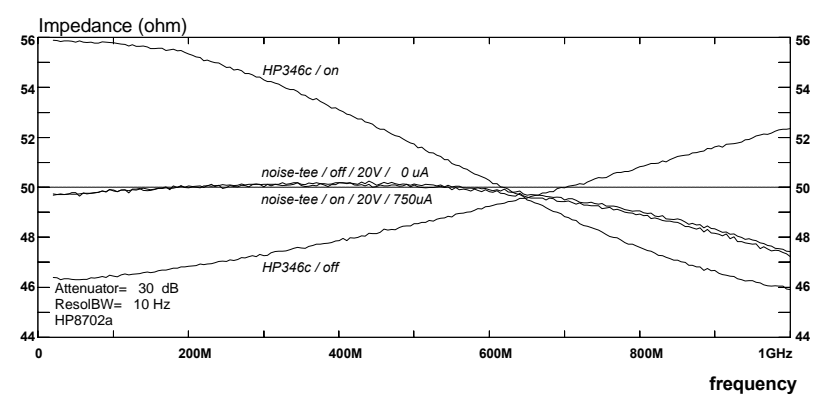


Fig 8.3 Output impedance measurements on a matched noise-tee configuration and a conventional noise source (HP346c), using 201 frequency points. One port is of the noise-tee is loaded with 50W. The output impedance of the other port is insensitive to variations of noise level, while variations of more than $\pm 10\%$ are observed for conventional noise sources.

As a matter of course, impedance variations of a noise source can be reduced by an additional matched attenuator or isolator. The attenuator reduces the excess-noise ratio, which restricts the measurement accuracy when the ENR is relatively small. The isolator reduces the usable noise bandwidth too, and thus the applicability of the noise source.

Furthermore it is observed that the output impedance of the noise-tee is (nearly) insensitive to variations of the noise-tee bias voltage, when it ranges from 5V to 20V. Nevertheless, the highest precision (e.g. less than 0.01 dB variation) will be obtained when the PIN photo-diode voltage is sensed and adjusted to a constant value with a dc feedback loop.

Another attractive feature is that the output impedance is variable over a wide range. This is performed by replacing the external load with a one-port impedance tuner. Fifty ohm calibrated noise sources require cascading with two-port tuners for similar impedance variation. This configuration blocks or shorts the signal flow when relative high or low impedances are required, which illustrates the advantage of our noise-tee configuration.

Figure 8.4 demonstrates how this is used in a setup that measures the input noise of an amplifier under test, at specified source impedance. The impedance tuner is adjusted in such a way that the output impedance of the noise-tee has the required source value. Note that this output impedance is frequency dependent, due to the internal transmission line of the noise-tee. As a result, the realization of the desired output impedance is often restricted to small frequency bands.

The output impedance of the noise-tee is variable over a wide range and is limited by the photo-diode capacitance, its bias network, and the internal transmission line. The highest values are obtained when photo-diode and impedance tuner are integrated with the amplifier chip (e.g. $0.2pF//100k\Omega$). To obtain a high output impedance at relatively low frequencies, e.g. below 100 MHz, the dimension of the transmission line in the noise-tee is of minor importance.

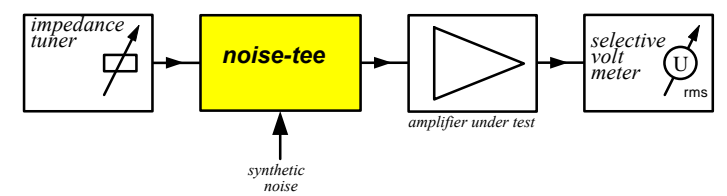


Fig 8.4 Mis-matched noise-tee configuration for noise measurements on an amplifier under test, at specified source impedance. The construction of this configuration is simpler than the combination of a two-port impedance tuner and a one-port noise source.

Another attractive feature of our noise-tee is that the mis-matched configuration of figure 8.4 facilitates the realization of 100% reflective sources (e.g. using an impedance tuner with infinite impedance). Examples are perfect shorts (0 Ω) perfect opens ($\infty \Omega$) and offset shorts and opens. When not in use, our noise-tee is equivalent with a pure transmission line, with no need to remove it.

This is a serious advantage, compared to conventional two-port impedance tuners. When a loss-free two-port tuner becomes 100% reflective, all available noise power from the noise source is blocked. This does not hold when source and tuner are reversed in position, however this requires an additional circulator.

Output impedances that are significantly different from 50Ω are attractive when measuring noise currents below the thermal noise level of 50Ω resistors. An example is the input noise current of an FET, especially at relatively low frequencies.

Commercially available setups for transistor noise parameter measurements, use 50Ω noise sources cascaded by a two-port impedance tuner. Since their output impedance is fixed, they require two-port impedance tuners to transform this impedance value to the desired value. At microwave frequencies, impedance transformation can be realized easily with resonating networks, however relatively low frequencies require other solutions, such as winded transformers.

As a result, the proposed setup in figure 8.4 is superior in simplicity, in competition with 50Ω calibrated noise sources and two-port impedance tuners.

8.2.5. Conclusions

In conclusion, it has been demonstrated that noise-tees, introduced in [802], have attractive additional features, compared to commonly 50Ω noise sources. Their noise level is easily varied over a wide dynamic range, while the associated noise level is accurately scaled from a calibrated reference value using simple dc-current measurements.

Furthermore the output impedance is mainly determined by an external impedance, and independent of the generated noise level. The mis-matched configuration of the noise-tee facilitates impedance tuning with one-port impedance tuners, while conventional methods require two-port tuners or circulators. Moreover, the mis-matched configuration facilitates a simple realization of 100% reflective sources. This is an advantage, compared to conventional two-port impedance tuners.

When not in use, our noise-tee is equivalent with a pure transmission line, with no need to remove it.

8.3. Calibration of synthetic noise

The measurement of noise, using white noise sources, requires a precise specification of the output noise level of the noise source. One way to perform this is to measure the spectral current density of the excess-noise current with an accurate frequency selective true-rms meter. More convenient methods use thermal noise or shot-noise as reference, because their values are based on fundamental physical constants. Thermal noise currents and shot-noise currents have the following well-known levels (single sided intensity spectra):

```
S_i = 4kT/R = level of thermal noise current of resistor R

S_i = 2q \cdot I_{dc} = level of shot-noise current of dc-current I_{dc}
                   k = (1.380662 \pm 0.000044) \cdot 10^{-23} \text{ [J/K]} Boltzmann constant
                    q = (1.6021892 \pm 0.0000046) \cdot 10^{-19} [C]
                                                                           Elementary charge
                    T = absolute\ temperature;\ 290[K]\ is\ the\ standard\ room\ temperature
                    S_i = (\text{single sided}) \text{ intensity spectrum of current } [A^2/Hz]
```

Thermal noise calibration may provide accurate results, however it requires a complex setup to heat and cool (50 Ω) resistors. The use of calibrated noise sources, such as an HP346c, is preferred as intermediate step when their calibration is traceable to a noise standard. Shot-noise calibration is superior in simplicity when lightwave (synthetic) noise sources are available.

This section describes novel calibration methods for lightwave synthetic noise using (1) calibrated noise sources or (2) shot-noise generated in illuminated PIN photo-diodes. The proposed methods are applicable to a wide range of noisy signals of lightwave origin, including RIN (relative intensity noise) of lasers and LED's.

8.3.1. Definition of (spectral) noise-current ratio for synthetic noise

Synthetic noise originates from the illumination of a PIN photo-diode, using a lightwave synthetic noise generator. The intensity spectrum S_i of the generated (random) photo current I(t) is frequency independent over a wide frequency band, and this property is referred as white noise. This noise is the uncorrelated combination of synthetic noise and shot-noise:

```
= dc-current; mean value of the random photo-current I(t)
S_{i,shot} = shot-noise level (2q·I_{dc}) associated with photo-current I_{dc}
S_{i,synth} = synthetic noise level, superposed on the photo-current I_{de}
S_{i,tot}^{i,synth} = total (excess) noise level: <math>S_{i,synth} + S_{i,shot} = S_{i,synth} + 2q \cdot I_{dc}
```

DC photo current I_{dc} is proportional to illuminated power, and the same applies for the amplitude of all ac terms superposed on that current. As a result, the ratio between amplitude spectrum ($\sqrt{S_{i \text{ synth}}}$) and the mean value (I_{dc}) of the photo-current is constant when the illumination is varied (see lightwave attenuator in figure 8.2). We define:

$$\mu \stackrel{\text{def}}{=} \frac{\sqrt{S_{i,synth}}}{I_{dc}} = \frac{\sqrt{S_{i,tot} - 2q \cdot I_{dc}}}{I_{dc}} = (spectral) \ noise \ current \ ratio$$

Calibration of synthetic noise is focused on the measurement of this constant μ . In this text, this constant will be referred as (spectral) *noise-current ratio* (NCR)³.

In [802], it has been demonstrated that this ratio is constant over a wide dynamic range. As a result, specification of μ and the measurement of I_{dc} facilitates the calculation of the noise level, using: $S_{i,tot} = (\mu \cdot I_{dc})^2 + 2q \cdot I_{dc} \approx (\mu \cdot I_{dc})^2$.

In most practical situations, the shot-noise $2q \cdot I_{dc}$ is negligible relative to the synthetic noise level. The bandwidth B is another characteristic constant of a synthetic noise generator, because approximately 50% of B is usable for white noise purposes (see section 9.2.3). In section 9.3.2 it will be demonstrated that B and μ are closely related for a well-designed synthetic noise generator:

$$\mu \approx \frac{1}{\sqrt{2 \cdot B}}$$

This approximation illustrates that shot-noise effects can be ignored when $I_{dc} \gg 2q/\mu^2 \approx 4q \cdot B$. For a 50 GHz synthetic noise generator this means that $I_{dc} \gg 0.03\mu A$. Since this condition is easily fulfilled, this text will further ignore this shot-noise side effect.

8.3.2. Calibration of synthetic noise with calibrated noise sources

Synthetic noise can be calibrated simply when it is injected in a matched noise-tee configuration. The generated photo current is exactly twice the output excess current when both electrical sides are equally matched to the characteristic impedance Z_0 of the noise-tee. The proposed calibration uses this property in a mis-matched noise-tee configuration, in which the load of one port is replaced by a calibrated noise source with equal output impedance Z_0 . Figure 8.5 shows the associated calibration setup, in which the lightwave synthetic noise is applied to the noise-tee as is illustrated in figure 8.2.

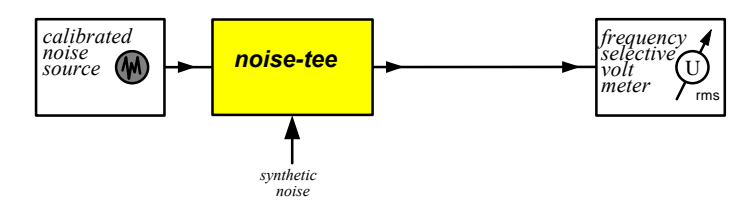


Fig 8.5 Noise-tee configuration for calibration of synthetic noise with a calibrated noise source.

R.F.M. van den Brink

 $^{^3}$ Our definition is closely related to that of laser RIN (relative intensity noise). RIN is commonly specified in dB/Hz using $10 \cdot \log_{10}(\mu^2)$. We used another name for μ since intensity noise is quite different from synthetic noise. Typical values for laser intensity noise and synthetic noise are -155 and -110 dB/Hz respectively.

The calibration is performed in two steps:

- In the first calibration state the calibrated noise source is activated, while the noise-tee is not illuminated. Since the noise-tee is nearly loss-free, the frequency selective voltmeter will detect the 'hot' noise level, which is accurately specified. This will be referred as the *calibration (noise) level*.
- In the second calibration state the calibrated noise source is switched-off, while the illumination of the noise-tee is switched on. The illumination level is adjusted by the optical attenuator (see figure 8.2) to make the output noise level equal to the (hot) level of the first calibration state. As a result the synthetic noise current has become equal to the (specified) excess-noise current of the calibrated noise source. This will be referred as the *reference (noise) level*, and the associated dc photo current as the *reference (dc) current* I_{d,ref}

Figure 8.6 shows the current flow for both calibration states.

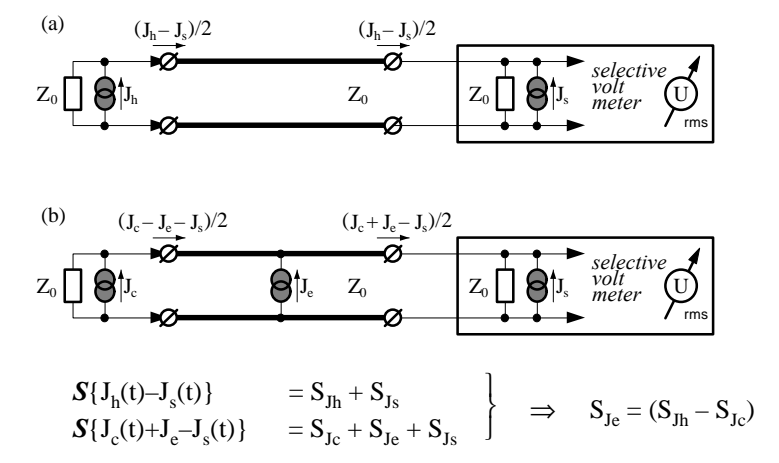


Fig 8.6 Current flow (time domain) of the various noise currents when (a) the source is on and the illumination is off, and (b) the reverse situation. In this model, the photo-diode capacitance is ignored. In our experimental noise-tee, this approximation is adequate up to 1 GHz.

The intensity spectrum S_{Je} of the synthetic noise current $J_e(t)$ equals the excess-noise current of the calibrated noise source, when both calibration states yield equal noise levels. As a result, the reference level equals a specified calibration level. The (spectral) noise-current ratio μ is the ratio of the *reference level* $\sqrt{S_{i,ref}} = \sqrt{S_{Je}}$ and the *reference current* $I_{d,ref}$.

Since the excess-noise current of the calibrated noise source is usually specified by an excess-noise ratio ξ (ENR), its value must be reconstructed using the standard room temperature (T_c =290K [817]) and the specified source impedance (R_0 =50 Ω):

$$\boxed{ \mu \stackrel{\text{def}}{=} \frac{\sqrt{S_{i,ref}}}{I_{d,ref}} \ = \ \frac{\sqrt{S_{Je}}}{I_{d,ref}} \ = \ \frac{\xi \cdot \sqrt{S_{Jc}}}{I_{d,ref}} \ = \ \xi \cdot \frac{\sqrt{4kT_c/R_0}}{I_{d,ref}} } \] } \ ENR = 20 \cdot log_{10}(\xi) \ [dB]$$

For example, assume a calibrated noise source, with R_0 =50 Ω output impedance, ξ =13dB excess-noise ratio, and room temperature T_c =290[K]. Furthermore assume that

the synthetic noise generates I_{d0} =20 μ A dc photo current while it equals the specified excess-noise. Then the various quantities are:

$$\begin{array}{lll} \xi &= 13 dB = 10^{13/20} \approx \sqrt{(19.95)} & \textit{excess-noise ratio} \\ S_{J_C} &= 4 k T_c / R_0 & \sqrt{S_{J_C}} \approx 18.1 \ pA / \sqrt{Hz} & \textit{cold noise} \\ S_{J_E} &= \xi^2 \cdot S_{J_C} & \sqrt{S_{J_E}} \approx 80.8 \ pA / \sqrt{Hz} & \textit{excess-noise} \\ S_{J_h} &= (\xi^2 + 1) \cdot S_{J_C} & \sqrt{S_{J_h}} \approx 82.8 \ pA / \sqrt{Hz} & \textit{hot noise} \\ \mu &= (\sqrt{S_{J_e}}) / I_{d0} \approx 4.0 \ (pA / \sqrt{Hz}) / (\mu A) \approx 1 / \sqrt{(2 \cdot 30.6 GHz)} \end{array}$$

The above equations presume a perfect match between noise-tee and its source and load impedance. As a result, a mismatch degrades the overall accuracy.

Using the theory on synthetic noise generation, as described in section 9.2.3 and 9.3.2, the value μ indicates that the noise bandwidth of the source was approximately $B\approx 1/(2\mu)^2=30.6$ GHz.



Fig 8.7 Illumination of a PIN photo-diode for shot-noise calibration. The light of a miniature lensed incandescent lamp is focused using a graded index lens, and inserted in he connectorized PIN photo-diode. See figure 8.8 for the associated setup of a shot-noise calibrator.

8.3.3. Calibration of synthetic noise, with shot-noise

The calibrated noise source of the calibration in subsection 8.3.2. is usually a thermal noise source or a calibrated noise source, initially calibrated with thermal noise. Shotnoise provides an attractive alternative.

The main advantage of our shot-noise calibrator is the high inherent accuracy when initial calibration with a primary noise standard is omitted. We observed corresponding results ($\approx 1 \text{dB}$ difference) between the method described in section 8.3.2 and this section

8.3.3. Further the construction of the proposed shot-noise calibrator is simple, compared to thermal noise sources. The shot-noise level is reconstructed from dc-current measurements, and slightly adjusted using an initial calibration. The ambient temperature and illumination level are irrelevant.

As early as 1943, Breazeale, Beers, Waltz and Kuper applied shot-noise calibration methods using temperature-limited vacuum diodes [203: page 273-278]. The dc current flowing through an illuminated photo-diode provides another known method to generate shot-noise. This approach is known from RIN-measurements, usually using a tungsten lamp [835]. We developed a simple shot-noise calibration setup [801,802] for synthetic noise, using a (reverse biased) PIN photo-diode illuminated with an incandescent lamp. The measured photo current provides the required calibration level.

Basic principle

The random fluctuation associated with dc photo current provides the desired shot-noise. When all the electrons cross the PIN-barrier independently and fully at random, then pure shot-noise will be provided. From this, the following prior conditions are concluded for the generation of *pure* shot-noise:

- Any additional random modulation of the illumination intensity must be avoided because it will exceed the spectral density of the photo current above its shot-noise level. As a result, the illumination must originate from a 'clean' light source. We assume that incandescent lamps are sufficiently 'clean' compared to other inaccuracy aspects. Other light sources, such as semiconductor lasers (and to some extend LED's) are not applicable, since their (unknown) RIN-levels (relative intensity noise) cannot be ignored unless it is proved. Some alternatives with balanced detectors are discussed at the end of this subsection.
- Any correlation between the moments that the electrons cross the barrier will prevent the noise from being pure shot-noise. This is a well-understood mechanism in space-charge limited vacuum diodes [720, p15], and quantified by a noise suppression factor Γ. For PIN photo-diodes a value of Γ=1 is commonly accepted, however, lower values [802] are observed (approximately 10% or 1 dB). To our opinion this is *not* the result of measurement errors (assumed to be better than 0.3 dB). Proving our measurement accuracy is an aspect of further interest. As a result, the intensity spectrum of the shot-noise current in the PIN photo-diode, originating from an incandescent lamp, equals: S_i = 2q·I_{d0}·Γ², with Γ≤1.

Figure 8.8 shows the proposed shot-noise calibrator⁴, shunted to a second PIN photodiode at the input of a low noise lightwave receiver. Using two diodes simplifies the construction One diode construction is optimized for receiving synthetic noise via an optical fiber, and the other is optimized for illumination with incandescent lamps. The construction with the lamp is shown in the photograph of figure 8.7.

We developed a dedicated receiver with capacitive current-current feedback (see chapter 6 or [608]) to meet the high performance requirements on noise and linearity, without loss of available bandwidth. Illumination with the lamp resulted in a dc photo current of approximately $I_{d0}{\approx}45\mu A$, which yields approximately $\sqrt{S_i}{\approx}3.8pA/\sqrt{Hz}$ shot-noise. For comparison, the thermal noise current of a 50Ω resistor at room temperature is

⁴ The shot noise was generated with a very small incandescent lamp (lensed, 100mW), which fits in the hole of an FC/PC connectorized photo diode. The diode of the experimental setup was an InGaAs/Inp planar PIN photo diode, (BT&D PDT0311: 1.2pF, 0.85A/W typical).

 $18pA/\sqrt{Hz}$. This illustrates how weak practical shot-noise sources are. The thermal noise current of a $1.1k\Omega$ resistor is approximately $3.8pA/\sqrt{Hz}$. As a result, the proposed shot-noise calibrator must be integrated with a low noise lightwave receiver, such as receivers with capacitive current-current feedback, as described in chapter 6.

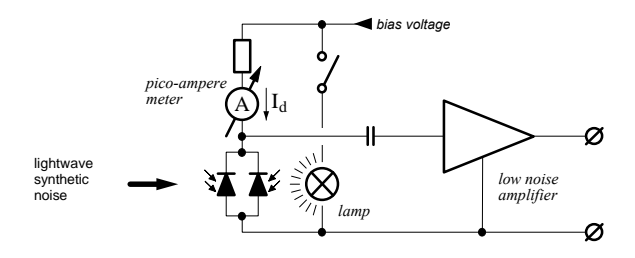


Fig 8.8 Circuit diagram of a shot-noise calibrator. The lamp illuminates a photo-diode and the resulting photo current is associated with shot-noise.

Calibration procedure

The shot-noise calibration is performed in two steps, similar to the noise calibration with a calibrated noise source and a noise-tee.

- In the first calibration state, the lamp is switched on while the lightwave synthetic noise generator is switched off. The resulting photo current is marked in this text as calibration current $I_{d,cal}$. The associated calibration level of the shot-noise is reconstructed from this dc current by calculation using $S_i = 2q \cdot I_{d0} \cdot \Gamma^2$.
- In the second calibration state, the lamp is switched off while the lightwave synthetic noise generator is switched on. The synthetic noise level is adjusted by an optical attenuator (see figure 8.2) to make the output noise level equal to the noise level of the first calibration state. As a result the synthetic noise level has become equal to the shot-noise level since both calibration states suffer from identical system noise contribution of the measurement setup. The resulting photo current is marked in this text as *reference current* I_{d ref}.

Figure 8.9a shows the measured output spectrum of the shot-noise calibrator. Since the receiver noise is uncorrelated with the shot-noise and synthetic noise, and the calibration level is known, reconstruction of the individual input spectra is feasible. Figure 8.9b shows the result, using the extraction algorithms of section 8.4.

The (spectral) noise-current ratio μ of the synthetic noise is the ratio of the reference level $\sqrt{S_{i,ref}}$ and the reference current $I_{d,ref}$ and has the following value:

$$\mu \, \stackrel{\text{\tiny def}}{=} \, \frac{\sqrt{S_{i,ref}}}{I_{d,ref}} \, = \, \frac{\sqrt{2q \cdot I_{d,cal} \cdot \Gamma^2}}{I_{d,ref}} \quad = \quad \Gamma \cdot \frac{\sqrt{2q \cdot I_{d,cal}}}{I_{d,ref}}$$

The advantage of shot-noise calibration is that the construction is simple. The dc-current meter is the only device that requires an absolute accuracy.

The assumption of $\Gamma=1$ provides fair results, however, values of $\Gamma\approx0.9$ are observed in the experimental setup. As a result, the noise level is 1 dB lower then was expected from pure shot-noise assumption. These are aspects of further investigations.

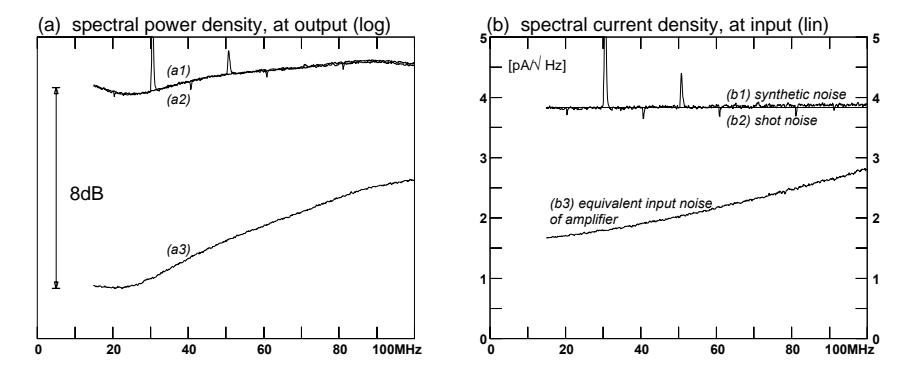


Fig 8.9 Measured output spectra (a) and reconstructed input spectra (b) of the shot-noise calibrator. The output spectra include the receiver noise and originate from (a1) lamp off, synthetic noise on, (a2) lamp on, synthetic noise off, and (a3) lamp off and synthetic noise off. The individual input spectra are unwrapped in figure b. The spikes originate from parasitic IM modulation in the synthetic noise source.

Illumination limitations

The excess-noise ratio (lamp on and lamp off) of the experimental shot-noise calibrator is relatively low. This is because shot-noise generators are in general weak noise sources. It is desired to increase the illumination, however this process suffers from principal limitations. This is summarized below:

- At first a photo-diode with low capacitance is required, to facilitate noise sources that are white over a sufficiently wide frequency band. Moreover, a low capacitance is crucial to facilitate low-noise amplification. Doubling the active area yields roughly doubling of capacitance and photo current, however the shot-noise increases with a factor √2. As a result, the active area of the PIN photo-diode must be chosen relatively small.
- Secondly the illumination originates from a (nearly) black-body radiator (hot filament of the incandescent lamp). This means that most of the optical power will not hit the active area of the photo-diode when projection methods with optical lenses⁵ are used. An optimal construction generates the desired photocurrent at minimal electrical lamp power, when the lamp temperature T is pre-defined.

The best that can be achieved is that all black-body radiation of an area is focused (with perfect optics) on an area A with equal dimensions. In practice, the power, collected over area A, is significantly lower due to imperfect lenses (see construction in figure 8.7). Moreover, the power radiated over area A is lower when the filament wire is thinner than the area diameter.

Light sources with higher power commonly use longer filaments. This means that the additional power will not hit the active area, and that light sources with more

(212) Lightwave based electrical noise measurements

R.F.M. van den Brink

⁵ It is possible that alternative projection methods based on integrating spheres yield better results. These alternatives are not investigated.

optical power may not necessary improve the overall result. Improvement of the optical coupling between lamp and diode, and increase of filament temperature (halogen lamp) is more effective.

 Thirdly, the responsivity of the photo-diode is wavelength limited. Since the spectrum of a black body radiator is usually wider, no more than a small part of the collected power is used for photo current generation.

The radiation law of Stefan-Boltzmann provides an expression for the maximum collected power P within an area A. The radiation law of Planck provides the spectral components $p(\lambda)$ of this collected power. This *maximum* is quantified by:

$$\begin{split} P &= \int_{0}^{\infty} p(\lambda) \cdot d\lambda = A \cdot \int_{0}^{\infty} \frac{(2\pi hc^2)/(\lambda^5)}{exp((hc)/(\lambda kT)) - 1} \cdot d\lambda = A \cdot \frac{2\pi^5 k^4}{15h^3c^2} \cdot T^4 = A \cdot \sigma \cdot T^4 \\ &\quad h = 6.626176 \cdot 10^{-34} \, [J \cdot s] \qquad \qquad Planck \ constant \\ &\quad c = 2.99792458 \cdot 10^8 \, [m/s] \qquad \qquad Speed \ of \ light \ in \ vacuum \\ &\quad k = 1.380662 \cdot 10^{-23} \, [J/K] \qquad \qquad Boltzmann \ constant \\ &\quad \sigma = 5.67032 \cdot 10^{-8} \, [W/(m^2 \cdot K^4)] \qquad Stefan-Boltzmann \ constant \end{split}$$

For example, consider a PIN photo-diode with d=70 μ m diameter, an active area of A= $\pi/4\cdot d^2$, and a filament with temperature T=2500 K. Then the collected illumination will not exceed the power level of P=8.5 mW. Furthermore assume a PIN photo-diode with a wavelength window of 1000 nm and 1600 nm, then approximately 32% of the collected power is used for photo current generation. This yields no more than 2 mA photo-current for a diode with 0.75 A/W sensitivity.

The maximum photo current, generated in our experimental setup with a miniature lensed lamp and an additional graded-index lens, was approximately 0.3 mA. This demonstrates that the shot-noise generator in the experimental setup is not optimal, however huge improvements are essentially impossible.

Alternative shot-noise sources

The unknown RIN (relative intensity noise) of LED's and lasers prevent them from direct use as shot-noise source in a shot-noise calibrator. The use of balanced receivers may facilitate an adequate suppression of the RIN of lasers [e.g. Kaspar et al: 805] and of LED's [e.g. Machida and Yamamoto: 806].

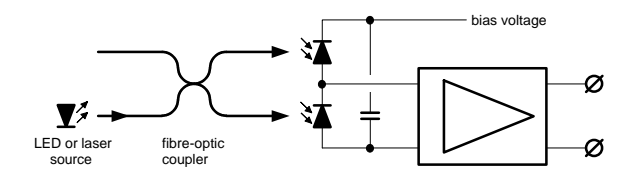


Fig 8.10 Balanced configuration to generate shot-noise with lightwave sources that suffer from RIN.

Figure 8.10 shows the basic configuration. The light beam of an LED or a laser source is coupled to a fiber and equally split in two beams. Each beam illuminates a photo-diode, and generates both shot-noise and RIN. Both magnitude and phase of the two branches are adjusted to perform perfect balance: equal beam splitting factor, equal fiber length and equal photo-diodes.

Since the RIN originates from the same light source, the associated noise currents in both diodes are fully correlated. As a result, the RIN is perfectly suppressed by subtraction. Since the shot-noise originates in the PIN photo-diodes, the associated noise currents in both diodes are fully uncorrelated. As a result, the intensity spectra of both shot-noise current sources increase by addition.

The balanced configuration may be used as an alternative for shot-noise generation with an incandescent lamp. However, it is not further discussed in this text.

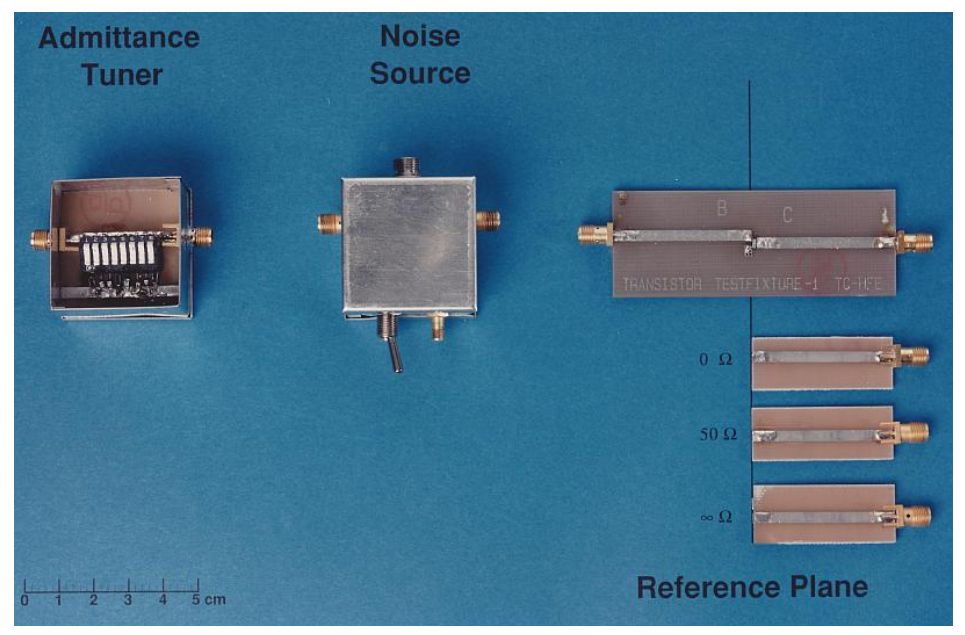


Fig 8.11 Practical setup for measuring noise, relative to an (arbitrary located) reference plane. In this example, a transistor is the amplifier under test, as illustrated in figure 8.12.

8.3.4. Transformation of calibrated noise to arbitrary reference planes

One of the most startling features of the noise-tee is the variation of output impedance with a simple one-port impedance tuner. When this impedance is known from impedance measurements, and shunted with a current source with white noise spectrum, then the spectrum of the noise voltage is easily extracted. However, the location of the output reference plane of the noise-tee does not coincide with the noise-tee photo-diode, which makes the intensity spectrum of the output noise subject to frequency variations. In the restricted case that one side of the noise-tee is matched to the characteristic impedance Z of the noise-tee, the synthetic noise spectrum is preserved at the noise-tee.

impedance Z_0 of the noise-tee, the synthetic noise spectrum is preserved at the noise-tee output (see figure 8.2). This makes the calibration of the previous subsections 8.3.2 and 8.3.3 directly applicable for noise measurements with fixed source impedances over a wide frequency range.

The general case of arbitrary reference planes requires an additional transformation of the noise from the diode reference plane to the chosen reference plane, by using the (measured) two-port parameters of the enclosed two-port. This subsection describes the required mathematics to perform this transformation.

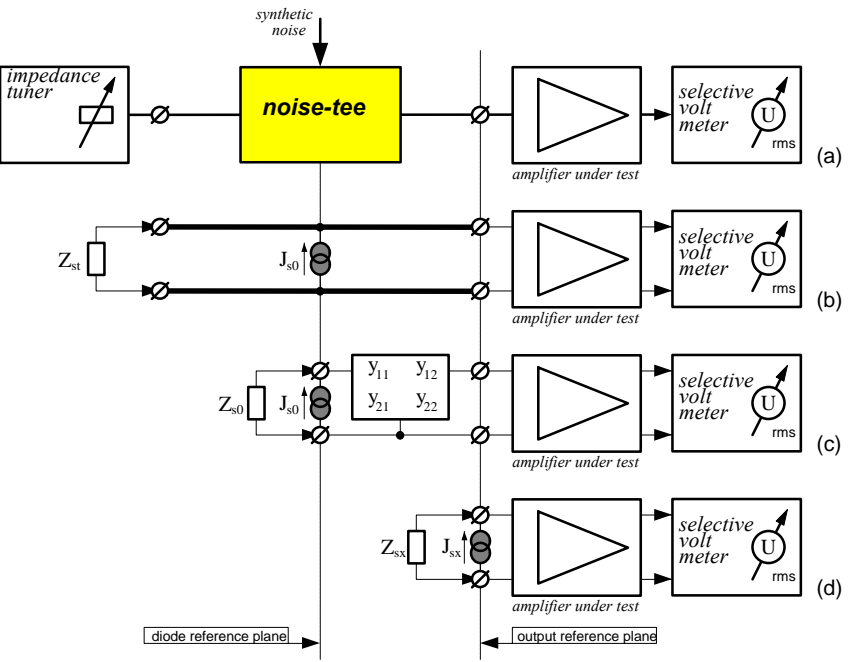


Fig 8.12 Mis-matched noise-tee configuration for noise measurements on amplifiers at specified source impedance.

Figure 8.12a shows a mis-matched noise-tee configuration to perform noise measurements on amplifiers at specified source impedance Z_{sx} . These measurements are of interest when the application of the amplifier under test is intended for sources with impedance Z_{sx} . The impedance tuner is adjusted to imitate that source impedance Z_{sx} of interest (observed at the output reference plane of the noise-tee).

Figure 8.12b shows the interior transmission line of the noise-tee that links the tuner impedance $Z_{st}(\omega)$ with the input of the amplifier under test. The (white) synthetic noise is represented by the (complex) noise current spectrum⁶ $J_{s0}(\omega)$. The (real) intensity spectrum $S_{Js}(\omega)$ of current $J_{s0}(\omega)$ is extracted by one of the previous discussed calibration methods (see section 7.1 for definitions).

Figure 8.12c shows the equivalent noise current spectrum $J_{sx}(\omega)$ that is the combination of synthetic noise and thermal noise, observed from the diode reference plane. The interior transmission line transforms tuner impedance Z_{st} into impedance Z_{s0} . Figure 8.12d shows the equivalent impedance and noise $Z_{sx}(\omega)$ and $J_{sx}(\omega)$, observed from the output reference plane. These values are to be extracted.

Assume that all two-port parameters of the right half of the noise-tee are known, for instance measured in s-parameter format. Transform them into y-parameter format for calculation convenience. Additionally assume the output impedance Z_{sz} is also known, e.g. by measurement. Using the general embedding and de-embedding equations of section 2.3.1, the transformations between J_{s0} and J_{sx} become:

$$J_{sx} = \left(\frac{-y_{21}}{Y_{s0} + y_{11}}\right) J_{s0} \qquad Y_{sx} = 1/Z_{sx} = \left(\frac{\Delta_{y} + Y_{s0} \cdot y_{21}}{Y_{s0} + y_{11}}\right) \\ J_{s0} = \left(\frac{y_{12}}{Y_{sx} - y_{22}}\right) J_{sx} \qquad Y_{s0} = 1/Z_{s0} = \left(\frac{\Delta_{y} - Y_{sx} \cdot y_{11}}{Y_{sx} - y_{22}}\right)$$
 \Rightarrow $J_{sx} = \left(\frac{Y_{sx} - y_{22}}{y_{12}}\right) \cdot J_{s0}$

The total hot level of the output noise is the composition of thermal noise (cold noise), due to tuner impedance and noise-tee losses, and the noise current spectrum J_{sx} (excess-noise). In a previous chapter, it is discussed that the intensity spectrum of a thermal noise current is easily extracted from admittance measurements. Since this cold noise current and excess-noise current are uncorrelated, and the (spectral) noise current ratio μ of the synthetic noise source is known, the various intensity spectra become:

$$\begin{array}{lll} S_{Js0,excess} &=& (\mu \cdot I_d)^2 & \text{originating from synthetic noise source} \\ S_{Js0,cold} &=& 4 \cdot kT \cdot \textit{real}(Y_{s0}) & \text{originating from thermal noise} \\ S_{Js0,hot} &=& 4 \cdot kT \cdot \textit{real}(Y_{s0}) + (\mu \cdot I_d)^2 & \text{total hot noise level at output reference plane} \end{array}$$

$$S_{Js0,hot} = (\mu \cdot I_d)^2 + 4 \cdot kT \cdot real \left\{ \frac{\Delta_y - Y_{sx} \cdot y_{11}}{Y_{sx} - y_{22}} \right\}$$
 observed at diode reference plane
$$S_{Jsx,hot} = (\mu \cdot I_d)^2 \cdot \left| \frac{Y_{sx} - y_{22}}{y_{12}} \right|^2 + 4 \cdot kT \cdot real(Y_{sx})$$
 observed at output reference plane observed at output reference plane

When both the diode reference plane and the output reference plane are (externally) accessible for measurement, then the transforming two-port parameters are extracted from two-port measurements. If not, the two-port parameters of the right half of the noise-tee must be made available from mathematical halving of the complete two-port. This is discussed in the succeeding subsection 8.3.5.

⁶ Complex noise spectra $J(\omega)$ are used only in intermediate results for calculation convenience, because they comprise amplitude as well as phase information. Since noisy signals are not deterministic by definition, phase information is not available, and amplitude information is restricted to a mean value in a small frequency band. Measurements are restricted to spectral power densities $S_J(\omega) = \langle |J(\omega)|^2 \rangle_{\Lambda\omega}$ of noisy signals.

8.3.5. Mathematical halving of the noise-tee

The two-port parameters of the internal sections of the noise-tee are not available by direct measurement, because the diode reference plane in figure 8.12 is inaccessible. Nevertheless, the symmetric two-port construction of the noise-tee facilitates another approach.

The noise-tee is a cascade of two identical but reversed two-ports, separated by the diode reference plane. When the overall cascade is measured, the internal sections may be extracted by a mathematical operation, similar to the 'root' of a matrix. An exact solution is essentially impossible, because a unique solution does not exist⁷. However, the most plausible solution is feasible in the case that an interior circuit model is available. The symmetrical construction of figure 8.1 and 8.14 is proposed to facilitate mathematical 'halving' of the noise-tee.

Figure 8.13 shows an equivalent circuit model of the internal noise-tee: a cascade of two transmission lines, that encloses a shunt impedance Z in the center. Due to imperfect balancing, the two transmission lines have different lengths. The shunt impedance represents the imperfect compensation of the diode capacitance by the micro strip slit (see figure 8.1).

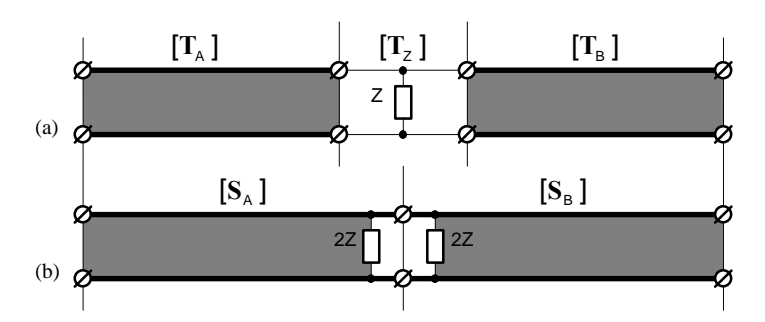


Fig 8.13 Equivalent circuit model of the noise-tee, to extract the halved two-ports from overall two-port measurements. In (a) the noise-tee is divided into three sections, while in (b) the shunt impedance Z is combined with the transmission line sections.

Figure 8.13a shows the cascade of idealized two-ports, using s-parameters rearranged in a transmission matrix. Let $x \stackrel{\text{def}}{=} \frac{1}{2} \cdot (Z_0/Z)$ be a shortcut to represent the shunt impedance, and let s_a and s_b represent the transmission of waves through the transmission lines. Then it can be demonstrated that the cascaded two-port has the following T-matrix and S-matrix form (see section 2.3.1 and appendix A):

$$\mathbf{T} = \mathbf{T}_{A} \cdot \mathbf{T}_{Z} \cdot \mathbf{T}_{B} = \begin{bmatrix} 1/s_{a} & 0 \\ 0 & s_{a} \end{bmatrix} \cdot \begin{bmatrix} 1-x & -x \\ x & 1+x \end{bmatrix} \cdot \begin{bmatrix} 1/s_{b} & 0 \\ 0 & s_{b} \end{bmatrix} = \begin{bmatrix} (s_{a} \cdot s_{b}) \cdot (1-x) & -(x) \cdot (s_{b}/s_{a}) \\ (s_{a}/s_{b}) \cdot (x) & (1+x) \cdot (s_{a} \cdot s_{b}) \end{bmatrix}$$

(217)

 $^{^{7}}$ The noise-tee is a symmetrical and reciprocal two-port, and is characterized by two unique complex numbers ($s_{11}=s_{22}$, and $s_{12}=s_{21}$). The mathematical halving must provide three unique complex numbers to represent its non-symmetrical halves. As a result, the set of two equations is incomplete to find a unique solution for three unknown.

$$\mathbf{S} = \begin{bmatrix} s_{11} & s_{12} \\ s_{21} & s_{22} \end{bmatrix} = \frac{1}{t_{11}} \cdot \begin{bmatrix} t_{21} & \Delta_t \\ 1 & -t_{12} \end{bmatrix} = \frac{1}{(1-x)} \cdot \begin{bmatrix} (s_a \cdot s_b) \cdot x & (s_a \cdot s_b) \\ (s_a \cdot s_b) & x \cdot (s_a \cdot s_b) \end{bmatrix}$$

The s-parameters of the (reciprocal) two-port are made available from measurements, which result in numerical values for x, s_a and s_b . Figure 8.13b shows how the shunt impedance is combined with the transmission line sections. The s-parameters of the scattering matrices \mathbf{S}_A and \mathbf{S}_B represent the two noise-tee sections:

$$\mathbf{S}_{A} = \frac{1}{(1-x/2)} \cdot \begin{bmatrix} (s_{a}^{2}) \cdot (x/2) & s_{a} \\ s_{a} & (x/2) \end{bmatrix}$$

$$using \begin{cases} \delta \stackrel{\text{def}}{=} (s_{b}/s_{a}) = \sqrt{(s_{22}/s_{11})} \approx 1 \\ x = \delta \cdot (s_{11}/s_{12}) \\ s_{a} = \sqrt{(s_{12} \cdot (1-x)/\delta)} = s_{b}/\delta \\ s_{b} = \sqrt{(s_{12} \cdot (1-x)/\delta)} = s_{a}/\delta \end{cases}$$

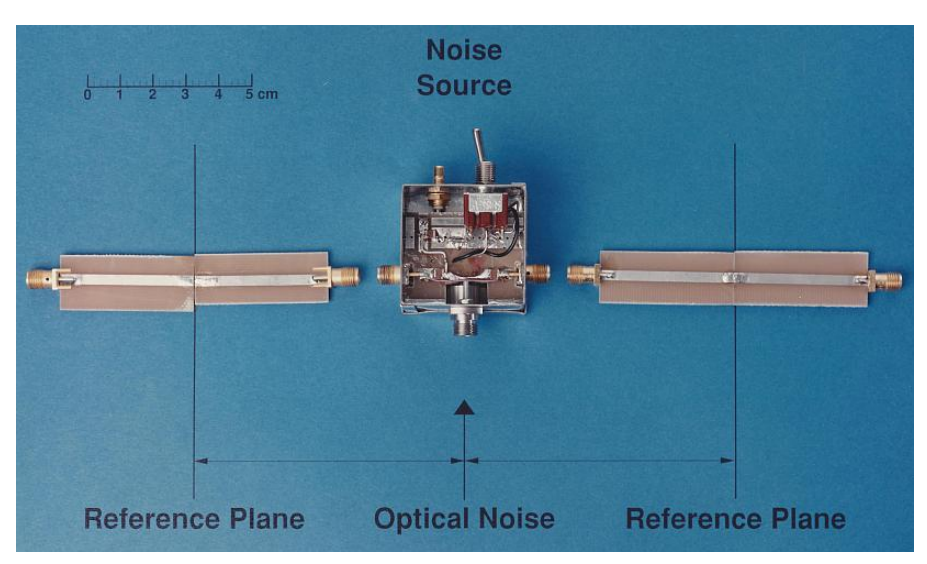


Fig 8.14 Mathematical halving of the lightwave noise-tee. The noise-tee is measured as electrical two-port, relative to external reference planes.

Practical aspects

The value δ represents the unbalance between the two sections. Its value is extracted from reflection measurements (s_{11} and s_{22}), however in well-designed noise-tees this

reflection is close to zero. As a result, the proposed extraction method for δ will yield unreliable results in case of low reflection values.

A fair solution is using an estimation for δ , e.g. by setting δ =1, based on the mechanical unbalance in the construction. More reliable values are obtained for δ from unbalance measurements using the photo-diode of the noise-tee (see figure 8.15). Modulate the illumination with a periodic signal, and detect the signal unbalance between the two output ports of the noise-tee. The (complex) ratio between both signals provides δ at the modulated frequency.

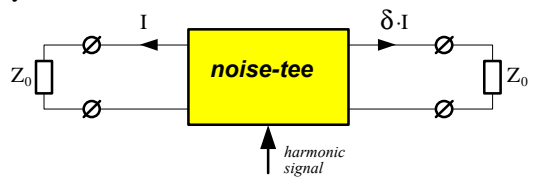


Fig 8.15 Noise-tee unbalance measurement using the lightwave input. The ratio d between both output currents is a measure for the unbalance between the two halves.

Another practical aspect is the sign uncertainty in the extraction of s_a and s_b . The root function has two solutions, and this may result in a sign uncertainty when wavelength is shorter than the noise-tee length. This is illustrated in figure 8.16. A reliable solution is obtained from phase unwrapping of s_a , using succeeding frequencies. The phase of s_a , as function of the frequency, has a saw-tooth shape. Add a multiple of the value π to this phase when it wraps, to make it a continuous function. The most reliable unwrapping is obtained when this decision is based on a transmission line model of the noise-tee, using line length and frequency information.

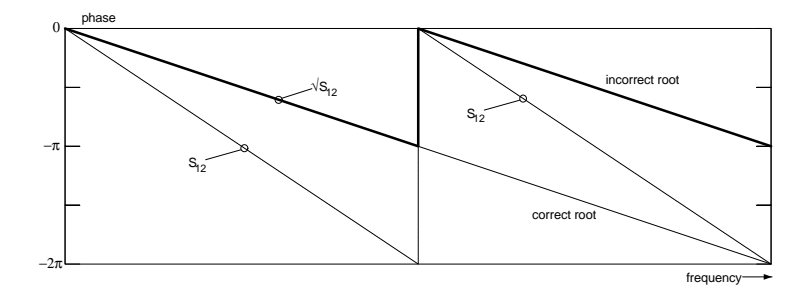


Fig 8.16 Sign uncertainty in the extraction of s_a and s_b . When the phase of s_{12} wraps from 2p to 0 then the phase of the root function $\ddot{\mathbf{O}}_{12}$ will wrap from p to 0. As a result, the sign of $\ddot{\mathbf{O}}_{12}$ swaps and yields an illegal value for s_a and s_b .

The extracted internal shunt impedance Z is indicative for the compensation performance of the diode capacitance by the micro strip slit (see figure 8.1). In the experimental noise-tee, the diode capacitance was reduced from 1 pF to below 0.3 pF, simply by removal of an empirically determined amount of copper. This demonstrates how effective the proposed compensation is.

The experimental noise-tee is based on a 50 Ω microstrip line, 3 mm wide and 38 mm long. The substrate is a standard glass-epoxy printed circuit board, 1.5 mm thick, 25 mm wide and 38 mm long.

8.3.6. Conclusions

Two convenient calibration methods for lightwave synthetic noise are demonstrated, using a (50 Ω) calibrated noise source and using shot-noise. Although the noise of the demonstrated shot-noise calibrator is significantly lower then thermal noise of 50 Ω resistors, the 'hot' shot-noise level is 8 dB higher then the 'cold' noise level. Furthermore, theoretical limitations are discussed of the maximum shot-noise level that incandescent lamps can generate in the proposed shot-noise calibrator.

The validation of the proposed calibration methods is restricted to reference planes that coincide with the PIN photo-diode in the noise-tee, unless both ports of the noise-tee are matched to its characteristic impedance. We demonstrated how to transform this calibration to arbitrary reference planes.

8.4. Noise level measurements using matched sources

The previous sections described various white noise sources and various methods to calibrate their noise level. This subsection applies these techniques to ratio noise measurements. A novel measurement method is described to measure the input noise of lightwave receivers, observed from an *optical* reference plane [801, 803]. To demonstrate its superior performance, our measurement method are compared with various alternative methods.

Ratio noise measurements with two calibrated noise levels (hot and cold) are commonly used for measurements on electrical receivers. Hence this section 8.4 is focused on multi-level noise measurements, applied to lightwave receivers.

This section describes a novel noise-extraction algorithm that takes the benefits of *multi-level* noise sources in ratio measurements. The proposed noise extraction algorithm minimizes the *relative*⁸ error in the reconstructed equivalent input noise levels. This provides the most plausible solution from detected output noise levels with comparative detection errors.

The section is restricted to noise sources, matched to the transmission line that links the source with the device under test. This restriction makes the noise position-*invariant*, which means that a location shift of the reference plane will not result in a noticeable chance of observed reference noise levels.

For electrical noise sources, this condition implies that the output impedance of the source is matched to the linking transmission line. As a result, the observed noise level as well as the source impedance are position invariant, observed from any reference plane between source and DUT (device under test).

For lightwave noise sources, this restriction implies that reflected waves are completely absorbed in the source. Furthermore it implies that the isolation between laser and fiber is adequate to prevent the laser from noticeable optical feedback effects.

The restriction of this section simplifies the measurement significantly. It makes complicated reference plane transformations, as described in section 8.3.4, superfluous. The more general case, with arbitrary mis-matched source impedances, is discussed in the succeeding section 8.5.

8.4.1. Basic principles and definitions

Figure 8.17 shows a block diagram of a ratio measurement setup. It starts with a (calibrated) variable noise source, generating (white) noise. The (single sided) intensity spectrum of the output noise level is set to reference input level S_r . The known noise level of the variable noise source as well as the unknown noise level of the device under test is amplified and detected with a frequency selective volt meter. The unknown system noise increases the detected voltage level.

_

⁸ The algorithms that we have found in the literature focus on the minimization of the absolute error (see section 8.5.1 on the state of the art). We assume that such an approach result in sub-optimal solutions, and that minimization of the relative error gives better performance.

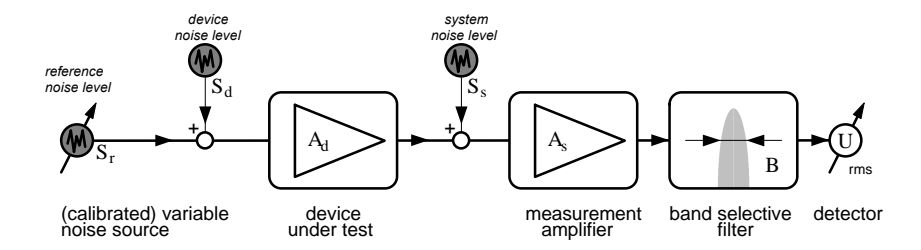


Fig 8.17 Block diagram of a ratio noise measurement setup. The device noise level is measured using calibrated noise. The gain of the device under test is unknown, and all sources are assumed to be uncorrelated.

 S_s = intensity spectrum of system equivalent input noise

 $S_d^{\rm s}$ = intensity spectrum of device equivalent input noise S_r = intensity spectrum of reference input noise

The detector detects the rms-voltage of the noise that has passed a selective band filter. It detects the values:

U_s when the device under test is switched off,

U_d when the device is activated but the variable noise source is switched off, and

 $\boldsymbol{U}_{\boldsymbol{r}}$ when the noise source as well as the device are activated,

All noise sources are assumed to be uncorrelated, which means that two noise currents add on a power base. As a result, the detected voltages are quantified by:

$$\begin{array}{ll} U_s \stackrel{\text{def}}{=} \sqrt{A_s^2 \cdot B \cdot S_s} & = \textit{detected system noise} \\ U_d \stackrel{\text{def}}{=} \sqrt{A_s^2 \cdot B \cdot S_s + (A_d \cdot A_s)^2 \cdot B \cdot S_d} & = \textit{detected device noise} \\ U_r \stackrel{\text{def}}{=} \sqrt{A_s^2 \cdot B \cdot S_s + (A_d \cdot A_s)^2 \cdot B \cdot S_d + (A_d \cdot A_s)^2 \cdot B \cdot S_r} & = \textit{detected reference noise} \end{array}$$

The device noise level S_d is extracted from the measured voltage levels $(U_s,\,U_d,\,U_r)$ and the reference noise level (S_e) by solving the above equations. When B and A_e are known, then the extraction process provides the device gain A_d too. To simplify these equations, we define:

$$\begin{array}{lll} G & \stackrel{\text{def}}{=} & (A_d \cdot A_s \cdot \sqrt{B})^2 & \textit{virtual power 'gain' of measurement setup} \\ S_{ds} & \stackrel{\text{def}}{=} & (S_d + S_s / A_d^2) & \textit{intensity spectrum of equivalent input noise} \\ P_s & \stackrel{\text{def}}{=} & U_s^2 & = & G \cdot (S_s / A_d^2) \\ P_d & \stackrel{\text{def}}{=} & U_d^2 & = & G \cdot (S_s / A_d^2 + S_d) & = & G \cdot (S_{ds}) \\ P_r & \stackrel{\text{def}}{=} & U_r^2 & = & G \cdot (S_s / A_d^2 + S_d + S_r) & = & G \cdot (S_{ds} + S_r) \end{array}$$

The measurement of voltage level U_d requires the variable noise source to be switched between 'on' and 'off'. When the device under test is a lightwave receiver, and thus the variable noise source must provide optical noise, then a perfect 'off' state exists. However, when the variable noise source must provide *electrical* noise, then the thermal noise of the noise source impedance limits the minimum reference noise level.

Simply removal of the noise source will affect the device noise level S_d and yields unpredictable results. This demonstrates that it is not self-evident that the value U_d is available for detection. As a result, when U_d is lacking then the extraction of the device noise level S_d requires at least two or more measurements of U_r , associated with different reference levels.

In the following sections, the required extraction algorithms will be discussed in more detail.

8.4.2. Extraction of input noise level using hot/cold noise sources

As early as 1953, IRE standards recommended [817,818,821] ratio noise measurements using two calibrated noise levels. The recommended method requires a variable noise source, of which the output noise level can be switched between 'high' and 'low' or rather between 'hot' and 'cold'. The restricted case of two reference levels (S_{r1} , S_{r2}), enables the use of a simple algorithm to extract the device spectrum S_d from the measurements (U_s , U_{r1} , U_{r2}). It can be demonstrated that:

$$G = \frac{S_{r2} - S_{r1}}{P_{r2} - P_{r1}}$$

$$S_{ds} = \frac{P_{r1} \cdot S_{r2} - P_{r2} \cdot S_{r1}}{P_{r2} - P_{r1}}$$

$$S_{d} = \frac{(P_{r1} - P_{s}) \cdot S_{r2} - (P_{r2} - P_{s}) \cdot S_{r1}}{P_{r2} - P_{r1}}$$

see section 8.4.1 for the definition of G, S and P.

The higher the ratio (S_{r2}/S_{r1}) is, the more precise S_d is extracted, provided that the device under test is not overloaded. Commonly specified values for the *excess-noise ratio* ¹⁰ (see section 8.1) of calibrated 50 Ω noise sources ranges from 5 dB to 20 dB. This means that (S_{r2}/S_{r1}) ranges from 2^2 to 10^2 . The 'cold' noise level is commonly the thermal noise of a 50 Ω resistor at the standard reference temperature T=290 K.

This method is often referred to as the Y-factor method, probably due to the ratio $Y=P_{r^2}/P_{r1}$ as used in formula 10 of [821].

8.4.3. Extraction of input noise level using multi-level noise sources

The choice of noise measurements with two noise levels is dictated by the limitations of commonly used electrical noise sources. The lightwave noise-tee, proposed in section 8.2, is much more flexible. Continuous variation of noise level is easy, without loss of accuracy or noticeable change of source impedance. This facilitates the use of more than one calibrated hot and cold noise level.

Multi-level noise measurements are attractive to reduce measurement errors by redundancy. Measurement errors are unavoidable, for instance quantization errors and distortion errors. Using more then two measurement levels, spread out over the dynamic

⁹ While measuring equivalent input noise, the noise source impedance must correspond with the signal source impedance for which the amplifier under test will be used. If not, the measured device noise will not correspond with the device noise under normal operation.

¹⁰ The excess noise ratio is defined (in dB) as ENR = $10 \cdot \log(S_{r2}/S_{r1}-1)$

range of interest, enables the extraction of a more plausible solution. That solution should spread errors out over all measurements, avoiding specific errors being improbably higher then all other errors. This approach may improve the overall measurement accuracy.

Conventional hot/cold measurements provide sets of equations having unique solutions. This does not hold for an over-determined set of equations, and the device noise extraction algorithm should select the most plausible solution.

A robust algorithm has been resulted from this study, that extracts S_d from multi-level measurements, optimized in a least-squares sense. Let the column vector $\boldsymbol{P_r} \!\!=\!\! [U_{rl}^{\ 2}, U_{r2}^{\ 2},, U_{rm}^{\ 2}]'$ represent the detected squared voltages U_r associated with the reference noise levels $\boldsymbol{S_r} \!\!=\!\! [S_{rl}, S_{r2},, S_{rm}]'.$ When more than two levels are measured then there will be no exact solution obtained for G and S_{ds} from the matrix equation: $\boldsymbol{P_r} = (S_{ds} + \boldsymbol{S_r}) \cdot G.$

All individual measurements P_{rx} are associated with a small deviation from the actual value. As a result, all expressions listed below are adequate.

$$\begin{split} G\cdot(S_{ds} \ + S_{rx}) &\approx P_{rx} \\ G\cdot(S_{ds} \ + S_{rx}) &= P_{rx} + \partial P_{x} \\ G\cdot(S_{ds} \ + S_{rx}) &= P_{rx} \cdot (1 + \delta_{x}) \end{split} \qquad \begin{array}{l} \partial P_{x} \ represents \ an \ absolute \ measurement \ error \\ \delta_{x} \ represents \ a \ relative \ measurement \ error \end{array}$$

An arbitrary solution can be found simply, by minimizing an arbitrary error (e.g. ∂P) with proper mathematics, however this will not necessary result in an optimal solution. Assume that the accuracy of the reference levels is superior, compared to the random measurement errors. Then, an optimal reconstruction of G and S_{ds} is associated with optimal *relative* accuracy for the reconstructed values $(S_{ds} + S_{rx})$. This yields optimal relative accuracy for $G \cdot (S_{ds} + S_{rx})$ which is equivalent with minimal (rms) average of the relative errors $\delta = [\delta_1, \delta_2,, \delta_n]'$. As a result, *equal* minimization of the errors ∂P_x will *not* yield the most plausible solution, while *equal* minimization of the errors δ_x will do. Now, the following matrix equation must hold:

$$\begin{bmatrix} P_{r_1} \cdot (1+\delta_1) \\ P_{r_2} \cdot (1+\delta_2) \\ \dots \\ P_m \cdot (1+\delta_n) \end{bmatrix} = G \cdot S_{ds} + G \cdot \begin{bmatrix} S_{r_1} \\ S_{r_2} \\ \dots \\ S_m \end{bmatrix}$$

$$\begin{bmatrix} 1+\delta_1 \\ 1+\delta_2 \\ \dots \\ 1+\delta_n \end{bmatrix} = \begin{bmatrix} 1/P_{r_1} & S_{r_1}/P_{r_1} \\ 1/P_{r_2} & S_{r_2}/P_{r_2} \\ \dots & \dots \\ 1/P_m & S_m/P_m \end{bmatrix} \cdot \begin{bmatrix} G \cdot S_{ds} \\ G \end{bmatrix} = \begin{bmatrix} 1/P_{r_1} & (S_{r_1}/S_0)/P_{r_1} \\ 1/P_{r_2} & (S_{r_2}/S_0)/P_{r_2} \\ \dots & \dots \\ 1/P_m & (S_m/S_0)/P_m \end{bmatrix} \cdot \begin{bmatrix} G \cdot S_{ds} \\ G \cdot S_0 \end{bmatrix}$$

 S_0 is an arbitrary scaling factor to reduce numerical roundoff errors. Optimal scaling is performed when S_0 is set to a value close to an average reference value S_r .

This matrix equation has $(1+\delta)=\mathbf{A}\cdot\mathbf{x}$ as general form. The most plausible solution vector \mathbf{x} must minimize vector $\mathbf{\delta}$, for instance in a least-squares sense. Using the overdetermined left-hand matrix division, as defined in appendix B, then a solution vector

 $x=A\setminus 1$ fulfills the requirement that the inner product $(\delta \delta')$ is minimized. This yields for the most plausible solution for G and S_{ds} :

$$\begin{bmatrix} G \cdot S_{ds} \\ G \cdot S_0 \end{bmatrix} = \begin{bmatrix} 1/P_{r_1} & (S_1/S_0)/P_{r_1} \\ 1/P_{r_2} & (S_2/S_0)/P_{r_2} \\ ... & ... \\ 1/P_{m} & (S_m/S_0)/P_{m} \end{bmatrix} \setminus \begin{bmatrix} 1 \\ 1 \\ 1 \end{bmatrix}$$

See section 8.4.1 for the definition of G, S and P. S_0 is an arbitrary scaling factor.

The scaling factor S_0 does not affect the solution, however a proper chosen value avoids round-off errors due to finite numerical precision. A good choice for this scaling factor is an arbitrary value, close to an average value of the reference levels S_r .

Error weighing

In the above equations, all levels are equal weighted. This means that an error in some level A is as important as another error in some level B. For example, when 90% of the measurements are performed at nearly equal levels and the remaining 10% at another level, than the above algorithm will favor the majority of the (correlated) errors at the expense of the minority. This is because the average error reduces when these (correlated) errors improve.

In this example, this effect is undesirable when all measurements were performed with equal accuracy, since it wrongly favors some specific levels. On the other hand, when the highest level is associated with the most erroneous measurement (e.g. distortion), then this effect may be crucial. The optimal solution for this effect is *weighing* of individual errors. It will relax the impact of individual errors on the overall accuracy.

Let $\mathbf{w}=[w_1,w_2,...w_n]$ be an appropriate set of weighing factors to define the desired minimization of $[w_1\cdot(S_{ds}+S_{r1}), w_2\cdot(S_{ds}+S_{r2}),, w_n\cdot(S_{ds}+S_{rn})]$. Then this minimization is equivalent with minimization of $[w_1\cdot\delta_1, w_2\cdot\delta_2,, w_n\cdot\delta_n]$. Using the same overdetermined left-hand matrix division as discussed before, it can be demonstrated that:

$$\begin{bmatrix} w_l \\ w_2 \\ \dots \\ w_n \end{bmatrix} + \begin{bmatrix} w_l \cdot \delta_1 \\ w_2 \cdot \delta_2 \\ \dots \\ w_l \cdot \delta_n \end{bmatrix} = \begin{bmatrix} w_l / P_{r_1} & (w_l / P_{r_l}) \cdot (S_r / S_0) \\ w_2 / P_{r_2} & (w_2 / P_{r_2}) \cdot (S_r / S_0) \\ \dots & \dots \\ w_n / P_{r_n} & (w_n / P_m) \cdot (S_m / S_0) \end{bmatrix} \cdot \begin{bmatrix} G \cdot S_{ds} \\ G \cdot S_0 \end{bmatrix}$$

$$\begin{bmatrix} G \cdot S_{ds} \\ G \cdot S_0 \end{bmatrix} = \begin{bmatrix} w_l / P_{r1} & (w_l / P_{r1}) \cdot (S_{r1} / S_0) \\ w_l / P_{r2} & (w_l / P_{r2}) \cdot (S_{r2} / S_0) \\ \dots & \dots \\ w_l / P_{rm} & (w_l / P_{rm}) \cdot (S_{rm} / S_0) \end{bmatrix} \setminus \begin{bmatrix} w_l \\ w_l \\ \dots \\ w_m \end{bmatrix}$$

See section 8.4.1 for the definition of G, S and P. S_0 is an arbitrary scaling factor. w_x are weighing factors

Set all weighing factors to an equal value, e.g. w=1, when all reference levels should equally pronounce in the reconstruction process. All specific levels with limited precision must be weighted with a lower value. A specific weighing value of $w_x=0$ will exclude a specific level.

8.4.4. Measurement of lightwave receiver noise

The input noise of the front-end receiver of an optical communication system is an important parameter for calculating the overall system sensitivity. Many lightwave receivers are reported in the literature, that focused on sensitivity improvement. Specification of the equivalent noise current (in pA/\sqrt{Hz}) is commonly used, to enable comparison with other reported receivers, or to claim new sensitivity records.

State of the art

Investigating commonly used noise measurement methods, we found no more than a few publications that mentioned their method to measure the receiver noise. The following methods were found:

- Direct noise measurements are often mentioned (see section 8.1). They measure output noise (usually with a spectrum analyzer), measure receiver gain or estimate it from what it should be, and reconstruct from these quantities the equivalent input noise [807, 808, 809, 810, 811, 812, 813, 814, 815].
- Kaspar et al. [805] compared equivalent input noise of a *balanced* receiver with white noise using a laser as light source. The balanced configuration facilitates suppression of laser RIN and the remaining noise level is (close to) the shot-noise level. This ratio calibration method has been discussed in section 8.3.3. In fact, they did not work out the method completely, however they enabled the reader to reconstruct the noise level from the ratio of the reported output spectra.
- Machida and Yamamoto [806] measured squeezing of light using a similar ratio noise measurement. They generated white noise in a balanced pair of photo-diodes using an LED light source (see section 8.3.3).
- Incidentally, the noise was not measured but estimated from specified noise parameters of the transistors that were used.

Most reported noise measurements did not mention how this noise level was measured. We assume that direct noise measurements are commonly used since instruments that facilitates lightwave ratio noise measurements are currently not commercially available.

Reliability of commonly used measurements

Most of the investigated papers did not indicate the reliability of the published values. The above overview is assumed to be indicative for the reliability of reported noise values since direct noise measurements suffer from poor accuracy performance. Many high-performance spectrum analyzers are specified with $\pm 2dB$ uncertainty for harmonic signals. Additional errors, that are associated with noise measurements, originate from uncertainties in noise correction, mismatch between receiver and instrument, and gain uncertainties.

The simplest noise correction divides the measured output noise spectrum by the root of the measurement bandwidth. Additional corrections up to 2dB are required for various noise corrections [804], however none of the above direct noise measurements mentioned what effects are taken into account, how these correction values were obtained and with what accuracy. This is relevant information since spectrum analyzers are not always equipped with specified noise markers.

Furthermore, we observed that it is no common use to specify what is measured. The information is usually restricted to the words noise power spectrum or noise intensity

spectrum simply the dimension [pAÖHz]. In section 7.1 a list of publications is summarized that demonstrates how different the words 'noise power spectrum' are interpreted by various authors. Sometimes it refers to the *single sided* noise intensity spectrum, while other authors meant *double sided* noise intensity spectrum. Both quantities are usually denoted with the symbol 'S', however they differ 3dB. This difference has been discussed in section 7.1.1. As a result, it is very difficult to intercompare the noise performance of various reported lightwave receivers. In this text, *single sided* noise intensity spectra are specified.

Ratio noise measurements with synthetic noise

Instruments for reliable electrical noise measurements are commercially available, however this holds not for lightwave noise measurements. In 1991, we proposed a novel ratio noise measurement method for lightwave receivers [801,803], using lightwave synthetic noise. This lightwave source is discussed in chapter 9.

Figure 8.18 illustrates the proposed measurement setup.

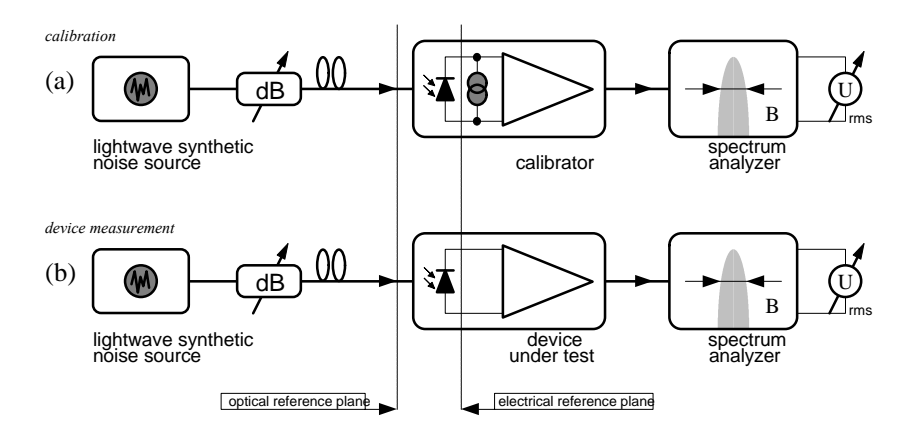


Fig 8.18 Block diagram of equivalent noise measurement on lightwave receivers. The synthetic noise is calibrated in (a) and then used in (b) to measure the ratio between the calibrated synthetic noise and the unknown device noise.

The first step in figure 8.18a is the calibration step, using one of the calibration procedures that are proposed in the section 8.3.2 and 8.3.3. In reference [801] shot-noise calibration with an incandescent lamp was used.

The calibration provides the spectral noise current ratio $\mu=(\sqrt{S_i})/(I_d)$, which is an inherent constant of the synthetic noise source. Subsequently, the optical power is adjusted to the desired power level for receiver noise measurement, using the lightwave attenuator. This optical power P_o is eventually measured with an optical power meter. When the photo-diode in the calibrator is also calibrated for optical power measurements, the optical power calibration can be integrated with calibration of the spectral noise current ratio μ .

The second step in figure 8.18b is the device measurement step, using calibrated synthetic noise to illuminate a receiver under test. Two reference planes are to be considered for noise specification:

- an optical reference plane at the optical input of the lightwave receiver, or
- an electrical reference plane at the output of the photo-diode.

The electrical reference plane is commonly used to specify the spectral *current noise density* $\sqrt{S_i}$ of the equivalent photo current (usually in pA/ \sqrt{Hz}). Its value is convenient in assessing the noise performance of the receiver pre-amplifier, but not of the lightwave receiver as a whole.

Noise specification observed from the optical reference plane is quite unorthodox, however it is more appropriate from a transmission system point of view. We will refer to it as lightwave *response noise density*¹¹ $\sqrt{S_o}$. Its level is proportional to $\sqrt{S_i}$ via the optical detector responsivity¹². The (scaled) dimension of $\sqrt{S_o}$ is $[pW/\sqrt{Hz}]$.

When P_{opt} is the optical power of the illumination, and when I_d is the dc photo current that is generated by that power, and when μ is the calibrated spectral noise current ratio of the synthetic noise source, then is the generated synthetic noise equal to:

$$\begin{array}{ll} \sqrt{S_o} &= \mu \cdot P_{opt} & \textit{observed from the optical reference plane} \\ \sqrt{S_i} &= \mu \cdot I_d & \textit{observed from the electrical reference plane} \end{array}$$

The optical power P_{opt} is always available for measurement, however the photo current I_d not. It is an internal signal of the device under test and requires receiver modification to make it external available. This is a significant advantage of specifying the lightwave response noise density. Furthermore, the synthetic noise is a white spectrum, observed from an *optical* reference plane. As a result, the unknown detector responsivity affects the spectral envelope of the synthetic current noise density $\sqrt{S_i}$. This illustrates that response noise density measurements are preferred to current noise density measurements.

Experiment

To demonstrate the reliability of ratio noise measurements with multi-level noise extraction, the equivalent input noise was measured of a lightwave receiver. Figure 8.19 shows the resulting spectra, observed from an output and an input reference plane. The output spectra in figure 8.19a represent the four reference output noise levels, as defined in section 8.4.1. They are the amplified levels of the combined device noise, synthetic noise and system noise.

The output spectra are frequency dependent since the receiver gain varies with the frequency. An additional ripple in the output spectra originates from mismatch errors between receiver and spectrum analyzer. These ripples change with the length of the linking cable, and will change when the receiver gain is measured with another instrument. This indicates that it would have been very difficult to correct for these mismatch effects when using direct noise measurements.

(228) Lightwave based electrical noise measurements

 $^{^{11}}$ The square S_{o} of the response noise density equals the noise equivalent power (NEP), normalized to 1 Hz noise equivalent bandwidth.

¹² The maximum responsivity of an arbitrary photo detector is restricted by physical constants: $r \le (q\lambda)/(hc)$. For $\lambda=1550$ nm, 1300nm and 850nm these limits are 1.250A/W, 1.049A/W and 0.686A/W respectively.

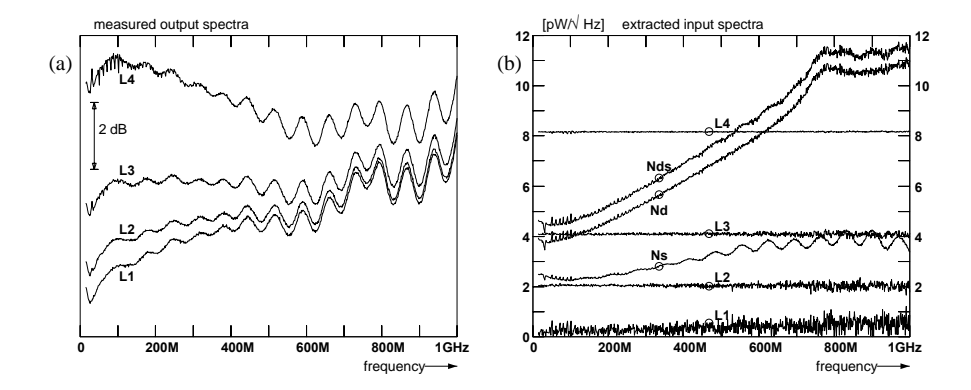


Fig 8.19 Measured noise spectra on electrical output (a) and optical input (b) of a lightwave receiver. The spectra L1 to L4 in plot (b) denote the levels of the synthetic noise source that are used as reference. The spectra L1 to L4 in plot (a) denote the detected output noise when the device is illuminated with these reference levels. The spectra N_d and N_s in plot (b) are the extracted device noise and system noise levels, observed from an optical reference plane. N_{ds} is the total equivalent input noise, resulting from the combination of N_d and N_s .

The equivalent input spectra in figure 8.19b represent various extracted noise levels, observed from an optical reference plane. Level L1 to L4 are the white synthetic noise levels, and were scaled from a calibrated level, using dc photo currents proportional to the illumination power. They were calculated from a multi-level extraction of virtual gain G and equivalent input noise $N_{ds} = \sqrt{S_{ds}}$, as defined in section 8.4.3.

All synthetic noise levels were equally weighted, assuming equally relative accuracy of the output spectra in figure 8.19a. As a result, the relative accuracy of the *extracted* synthetic noise levels degrades for very low illumination levels (note level L1 in figure 8.19b). These are realistic consequences.

The robustness of the multi-level extraction method has resulted in complete disappearance of the mismatch ripple in the spectra that originates at the input. This does not hold for the system noise $N_s = (\sqrt{S_s})/A$, since that noise is generated at the receiver output. Figure 8.19b demonstrates that the levels N_s and N_{ds} have some ripple, however it has disappeared in the device noise level $N_d = \sqrt{S_d}$. These are realistic results.

As a result, these experiments demonstrate the validation of the new multi-level extraction method, as proposed in section 8.4.3. The relative accuracy of the proposed noise measurement method on lightwave receivers is superior to the commonly used direct noise measurement. Conventional methods are usually unable to eliminate ripple effects that do not belong to the equivalent noise that is measured.

The absolute accuracy is mainly restricted by the accuracy of a common scaling factor. This means that all extracted levels are in equal proportion too high or too low. The uncertainty of dc optical power measurements takes the greater part of this (small) scaling error.

Furthermore, the proposed method provides gain information simultaneously, can be carried out simply, and results in noise measurements observed from an optical reference plane.

8.4.5. Alternative lightwave receiver noise measurements

Additional gain measurements facilitate the transformation of the equivalent input noise from the optical to the electrical reference plane and reverse. The property that our ratio measurement method extracts the noise at the *optical* reference plane, without additional gain measurements, is a non-trivial property. Most alternative ratio measurements extract the noise at an electrical reference plane. To demonstrate various superior performance aspects, our ratio measurement method is compared with alternative ratio methods.

- (1) An alternative ratio method is electrical measurement of the four *noise parameters* of the receiver pre-amplifier. These parameters facilitate the reconstruction of equivalent input noise when the pre-amplifier is combined with the photo-diode. Although they require modification of the receiver under test to get access to internal reference planes, they are applicable. Automated measurement setups, using 50Ω noise sources and impedance tuners are commercially available.
- \Rightarrow We assume that these cumbrous and sophisticated methods suffer from poor accuracy performance. The output impedance of photo-diodes is relatively high, which enables the design of very low-noise pre-amplifiers. This causes that the equivalent input noise is often significantly lower than the thermal noise of 50Ω resistors. Since this level is significant lower than the cold noise level of 50Ω measurement methods (18pA/ $\sqrt{\text{Hz}}$), we assume that the noise extraction will be inaccurate.
- (2) A variant to the previous ratio method originates from using high-impedance *thermal noise* sources. Insertion and removal of various resistors, shunted to the photo-diode, may facilitate the extraction of equivalent input noise from thermal noise levels. The intention of the method is to avoid removal of the photo-diode and to avoid accurate impedance measurements.
- ⇒ At the beginning of our study to noise measurements, some experiments with this approach were performed, yielding poor results. The insertion of shunt impedances to the input affects the amplifier gain. Furthermore the equivalent device noise change with this impedance. This is a relevant problem, since the insertion of sufficiently high resistors is associated with noise levels that are too low for convenient noise measurements (see figure 8.20). Using four or more impedance values facilitates the extraction of all four noise parameters. This requires, however, the insertion of real as well as complex impedances. The RF-impedance of pure resistors is known from dc measurements with fair accuracy, however, insertion of very small capacitors requires impedance measurements at well-defined reference planes. This annihilates the simplism of the method, and requires an approach as is discussed in (1).
- (3) The use of *shot-noise*, generated by an incandescent lamp, is well applicable under restricted conditions. This method is very similar to the shot-noise calibration previously

illustrated in figure 8.8. The calibration and the measurement, however, are simultaneously performed in the receiver under test.

⇒ This approach is restricted to receivers that gives access to internal photo currents for extracting the shot-noise level from dc measurements. Furthermore the method is restricted to receivers with open or connectorized photo-diodes. Pigtailed¹³ photo-diodes are hardly applicable, since that fiber is an impediment for adequate coupling of incandescent light.

Shot-noise methods require bright illuminations to generate adequate shot-noise levels. The associated dc photo current may overload the receiver under test by impeding the receiver biasing. Figure 8.20 demonstrates the superiority of synthetic noise, compared to shot-noise, on generation of dc offset currents. Shot-noise calibrators (see section 8.3.3) may be optimized for these high offset currents, since their bandwidth performance is irrelevant. This does not hold for all dedicated low-noise receivers under test, which restricts the application of the method.

	$\sqrt{S_i}$	=	1 pA/√Hz	3 pA/√Hz	10 pA/√Hz
thermal noise	$R = 4kT/S_i$	=	16.4 kΩ	$1.82 \text{ k}\Omega$	164 Ω
shot-noise	$I_{dc} = S_i/(2q)$	=	3.12 μΑ	28.1 μΑ	312 μΑ
synthetic noise (B=50 GHz)	$I_{dc} \approx \sqrt{(2B \cdot S_i)}$	≈	0.32 μΑ	0.95 μΑ	3.16 µA

Fig 8.20 Comparison of the resistors or the dc currents that are associated with the generation of thermal, shot or synthetic noise. Synthetic noise combines a minimum in dc current with a maximum in noise level.

(4) Using *shot-noise* in combination with *balanced receivers* is also well applicable under restricted conditions. This method is very similar to the shot-noise calibration previously illustrated in figure 8.10. The balanced configuration avoids dc offset currents, since the photo current supplied by one diode is drained away by the other.

The method enables the use of LED and laser sources, to avoid coupling problems in pigtailed receivers. Care must be used in this measurement technique to obtain reliable results. The balancing must adequately suppress the undesired RIN below the shot-noise level to facilitate reliable shot-noise calibration. Kaspar et al. [805] reported the use of a laser source and Machida and Yamamoto [806] an LED source.

- ⇒ Although the method is very well applicable for balanced receivers, it requires access to internal photo currents for extracting the shot-noise level from dc measurements. The method is not applicable to other type of receivers.
- (5) The use of *intensity noise*, that is modulated on the output power of a light source, is an alternative for synthetic noise. Explicit electrical modulation may be omitted when the RIN levels of lasers or LED's are adequate. This approach is very similar to our synthetic noise method, since it requires additional calibration and is applicable to a

¹³ For the ease of connecting to a fiber, some manufacturers supply LEDs, lasers and photodiodes with a short length of fiber, called pigtail.

wide range of receiver classes. It is the first method in this list that facilitates noise specification at an optical reference plane, without additional gain measurements.

⇒ The weak point of this approach is its calibration, since the spectral envelope of intensity noise is not white. The RIN curve of lasers is related to the electrical to optical transfer function and increases with the frequency up to the relaxation frequency of the laser. Typical values comprise several dB's up to a few GHz.

As a result, the calibration is required over the full frequency band of interest, which introduces many uncertainties due to unknown frequency responses in the calibration setup. Synthetic noise is white, up to tens, probably hundreds of GHz, which enables a simple calibration at relatively low frequencies.

- (6) Our synthetic noise source is not the only lightwave signal, that generates white noise when it illuminates a photo-diode. Other examples are lightwave signals originating from *spontaneous emission*. Eichen et al. [816] proposed bandwidth measurements on lightwave receivers using amplified spontaneous emission from semiconductor optical amplifiers.
- \Rightarrow Whatever spontaneous emission source is used, their enormous spectral width makes them inferior to synthetic noise, with respect to dc-offset currents. A synthetic noise generator concentrates all available power in a bandwidth B that is selected by the user (see section 9.2.3). The more this power is spread out over a huge bandwidth, e.g. more than $5 \cdot 10^{12}$ Hz, the lower the usable spectral density will be. Measurements up to 100GHz would utilize only the first 2% of the width [816]. Since photo currents are proportional to the illuminated power, the associated dc photo current is significantly higher than was associated with synthetic noise for equal noise level.

The performance of spontaneous emission signals, with respect to dc offset current, is somewhere between the performance of synthetic noise and shot-noise.

8.4.6. Conclusions

In conclusion, a novel algorithm is developed for extracting equivalent input noise from multi-level noise measurements. This approach reduces random measurement errors by redundancy. Our algorithm minimizes the *relative* measurement error in a least-squares sense.

A new measurement method is proposed for measuring lightwave receiver noise. The method uses a new device, a synthetic noise source, a new multi-level extraction algorithm and dedicated calibration techniques to perform reliable ratio noise measurements over very wide frequency bands.

The high relative accuracy of our method is demonstrated. The absolute accuracy is mainly restricted by the accuracy of a common scaling factor. The uncertainty of dc optical power measurements takes the greater part in this (small) scaling error, followed by the accuracy of the calibrated noise level in the calibrator.

Our method is compared with various alternative methods for demonstrating its superior performance. The proposed method facilitates specification of noise at an *optical* input reference plane. It can be performed simply and is applicable to a wide range of lightwave receiver types.

8.5. Noise parameter measurements

A practical noise measurement setup requires the connection of a noise source to a DUT (device under test) via a transmission line, such as coaxial cables, wave guides or fibers. The previous section was restricted to sources that absorb all reflections to the DUT. As a result, the noise source was virtually located in any reference plane between source and DUT. A location shift of the reference plane requires no more than an amplitude correction of the source level due to (minor) transmission line losses. This simplified the noise extraction from the measurements significantly.

When the source admittance changes, the source becomes mis-matched. A location shift in reference plane will then require correction for source level as well as source admittance. Furthermore, the input excess-noise varies with the source admittance too. This makes that the measurement is preferably performed with a noise source that has a similar source admittance. As a result the noise extraction from the various measurements is complicated when the source admittances are mis-matched.

These difficulties are characteristic for electrical applications, and are not relevant for common optical applications. When a similar source admittance is not available, the preferred approach is different. All four noise parameters of the DUT have to be measured and the noise for the requested source admittance have to be reconstructed from these parameters.

This section starts with the state of the art in two-port noise parameter measurements. Various improvements will be summarized that result from replacing conventional 50 Ω noise sources with our noise-tees in state-of-the-art noise measurements.

A novel algorithm will be propose that generalizes two-port noise parameter extraction of a device under test, when its input impedance is known. The algorithm holds for any combination of noise sources, each with arbitrary effective 'temperature' and impedance. When more then five sources are used, the algorithm extracts the most plausible solution, by minimizing the *relative* error.

This section demonstrates that our opto-electronic methods and algorithms are capable of noise measurements with distinct (mis-matched) source admittance, and of extraction of all two-port noise parameters.

8.5.1. State-of-the-art measurement methods

Most noise parameter measurements rely on noise figure measurements, on historical grounds. Its definition is related to the noise power delivered to the output, when a *device under test* (DUT) amplifies the thermal noise of a passive source admittance. By definition [817] it is the ratio between (1) the actual output power and (2) the output power when the DUT would have been noise free. When F=1, the DUT is noise free; when F=2, the input noise equals the thermal noise of the source admittance. As a result, the equivalent input noise spectra, that are associated with that resistance 14, have the following intensities:

(233)

 $^{^{14}}$ R is a chosen reference resistance, usually 50Ω , and T is a reference temperature. The IRE standard reference temperature [817] is defined as T=290K.

```
\begin{array}{lll} S_{i,hot} &= (4kT/R) \cdot F &= \text{hot noise level of equivalent input noise current} \\ S_{u,hot} &= (4kT\cdot R) \cdot F &= \text{hot noise level of equivalent input noise voltage} \\ S_{i,excess} &= (4kT/R) \cdot (F-1) &= \text{noise current, in excess to the thermal noise of the source} \\ S_{u,excess} &= (4kT\cdot R) \cdot (F-1) &= \text{noise voltage, in excess} \text{ to the thermal noise of the source} \\ S_{i,cold} &= (4kT/R) &= \text{cold noise level due to thermal noise current of the source} \\ S_{u,cold} &= (4kT\cdot R) &= \text{cold noise level due to thermal noise voltage of the source} \\ \end{array}
```

The noise factor (or noise figure), is convenient in a 'transmission line environment' where all devices are designed for operation at equal source and load admittances. The definition is meaningless when the admittance (or impedance) of the input termination is not specified. To our opinion, the use of noise factor F for 50Ω is very inconvenient when amplifying signals generated by ideal voltage or current sources (such as photodiodes).

The measurement of noise factor F at a distinct source admittance requires a calibrated noise source connected to the DUT. A tunable network between source and DUT facilitates the adjustment of the admittance of interest. Then the output noise is detected, and F is measured via ratio methods. This method is often referred as the Y-factor method, probably due to formula 10 in [821]. The use of automated noise figure meters, that controls the 'hot' and 'cold' states of the noise source, is more preferred.

The noise factor F varies with source admittance Y, and Rothe and Dahlke [713] published in 1956 a simple four-parameter expression¹⁵. For a nice overview of this theory, see Hartmann [722] with many relevant references.

At a specific source admittance (Y_{opt}) , the noise factor is minimal (F_{min}) . Most noise parameter measurements are focused on the extraction of these parameters, and an additional scaling factor R_n : $[F_{min}, \textit{Re}(Y_{opt}), \textit{Im}(Y_{opt}), R_n]$ (see chapter 7). These four (real) parameters can be transformed into any form of interest, using the theory of chapter 7.

Paired hot and cold noise measurements, with search to F_{min}

- (1) The classic approach, recommended since 1960 by the IRE [818,819,820,821], uses a loss free tuner (a variable-ratio transformer or a movable stub tuner). At each admittance of interest, the noise figure is measured with hot/cold ratio measurements. The admittance is adjusted, using trial and error methods, to find a minimum readout F_{min} for the noise figure. The associated source admittance provides a specific value Y_{opt}. The value R_n is then calculated from a previously measured pair of (F, Y), or extracted from all measured pairs (F, Y) using a graphic linear regression method.
 - Lange [822] proposed in 1967 an alternative noise parameter $N \stackrel{\text{def}}{=} R_n \cdot Re(Y_{opt})$, as replacement for R_n . He demonstrated that N as well as F_{min} are invariant under lossless transformation. Y_{opt} transforms through a lossless two-port like any admittance. This illustrates that F_{min} and N are fundamental properties of the DUT in transmission line operation. Therefore the admittance Y_s can be measured at the

$$15 \ \text{Noise figure:} \quad F \ = \ F(Y) \ = \ F_{\text{min}} \ + \ \frac{R_{\text{n}}}{\textit{Re}(Y)} \cdot |Y - Y_{\text{opt}}|^2 \ = \ F_{\text{min}} \ + \ N \cdot \frac{|Y - Y_{\text{opt}}|^2}{\textit{Re}(Y) \cdot \textit{Re}(Y_{\text{opt}})}$$

most convenient reference plane located between the two-port under test and the noise source, with no effects on N and F_{min} . They are terminal invariant in a lossless region, and Y_s is the only parameter to be transformed.

Paired hot and cold noise measurements, with curve fitting

- (2) The drawback of method 1 is that the tuner must provide all admittance values of interest. The optimal admittance was found on a trial and error base, guided by manual curve fitting techniques.
 - Lane [823] was the first to introduce in 1969 an algebraic fitting approach on measured pairs of (F,Y) for discrete admittance values (four or more). He transformed that expression into a linear form to extract the desired parameters from an over-determined set of simultaneous equations. Caruso and Sannino [827] improved the accuracy in 1978, using properly chosen source admittance values. Both methods [823,827] minimize the absolute error ΔF in F in a least-squares sense, to improve the overall measurement accuracy (one-dimensional minimization).
 - \bullet Mitama and Katoh [828] improved in 1979 the curve fitting method, using a three-dimensional minimization. They minimized the combined absolute error $(\Delta F^2 + \Delta Y^2)$ in an iterative approach.

Arbitrary hot and cold noise measurements, using input admittance.

- (3) The drawback of methods 1 and 2 is that at least eight output noise measurements are required: four pairs of 'hot' and 'cold' measurements. Furthermore, method 1 and 2 require that the source admittance does not change with the effective 'temperature' of the source. More economical methods make use of additional information on the input admittance. This relaxes the requirement to perform the measurements in pairs with equal source admittance, and reduces the number of noise measurements.
 - Engen [824] proposed in 1970 a method with four noise measurements and an input admittance measurement. He measured the output noise levels (P_{oh}, P_{oc}) associated with a matched hot/cold source, the output noise levels (P_{oM}, P_{om}) associated with a sliding short adjusted at maximum/minimum output level.
 - Adamian and Uhlir [825,830] proposed in 1973 a method with five noise measurements and an input admittance measurement: one pair of hot/cold measurements with a noise source, and three additional cold measurements at arbitrary source admittance values. They considered that different admittances are allowed for the noise source in the 'hot' and 'cold' state, and suggested an iterative approach to use this information in the noise parameter extraction.

Davidson et al. [831] proposed in 1989 a non-iterative correction method for variation in source admittance when varying the noise 'temperature'. They demonstrated the advantages when the measurements are corrected for these effects. As a result, it is not necessary to measure cold noise power at the source admittance produced by the hot source.

Equal temperature noise measurements

(4) Probably the most convenient measurement method is a method that uses 'cold' measurement only, or have at least all sources at equal 'temperature'.

• Gupta [829] demonstrated in 1983 that such a solution does not exist when the output noise power is the only measured quantity.

Multi-port noise measurements, using N-port parameters

- (5) All previous methods use switched or tunable input impedances to extract the four noise parameters of the DUT. This is a disadvantage when the measurement frequency ranges over several decades.
 - Wedge and Rutledge [833] proposed in 1992 a two-port method that performs simultaneous measurements of the noise waves that emanate from input and output ports of the DUT. The proposed setup uses two noise sources to perform ratio measurements on the noise waves originating from port 1, originating from port 2, and a mix of both waves using 90° and 180° hybrids. Transformation of all noise contributions to equivalent input values requires the measurement of the all twoport parameters of the DUT.

The multi-port noise measurement requires additional two-port parameter measurements to extract the *input* noise parameters. The distinct hot and cold noise measurement requires an additional input admittance measurement on the DUT. When the input admittance is not available for measurement, then the paired hot and cold noise measurements apply.

Automated methods, using hot and cold measurements, are commercially available. They use electrical noise sources (50 Ω), in combination with automated tuners or switched admittances. Two-port tuners are commonly used for the paired hot and cold noise measurements, however additional circulators facilitate the application of one-port tuners.

8.5.2. Proposed improvements to state-of-the-art noise measurements

Most state-of-the-art methods of the previous section are reliable methods. Nevertheless, there is still room for improvement. This subsection summarizes various improvements that result from replacing conventional 50Ω noise sources with our noise-tees, and that result from our new noise extraction algorithms.

All reflective source

- (–) The paired hot/cold measurements require noise generators with variable source admittance. Conventional methods (50Ω source, two-port tuner) must be content with limited tuning ranges for admittance values since high reflective sources (shorts, opens, offset shorts, etc.) are associated with very low noise levels.
- (+) Our noise-tee is a *two-port* device, and requires no more than a one-port admittance tuner. An offset short on one port will result in a 100% reflective source for all frequencies, but will not block all available noise power. This makes our noise-tee wider applicable than 50Ω noise sources.

Invariant source admittance

- (–) Paired hot/cold measurements require noise generators with source admittances invariant under effective 'temperature' variations. Section 8.2.4 demonstrated that commercially available sources are liable up to 10% variation of output admittance.
- (+) The admittance of our noise-tee is highly insensitive to variation of noise level.

Zero cold level

- (–) Paired hot/cold measurements, using conventional 50 Ω noise sources, are associated with a minimum 'cold' noise level. The thermal noise of the cold 50 Ω resistor restricts the measurement accuracy on very weak noise currents, especially when their level is significant lower than the 'cold' level of 18 pA/ $\sqrt{\text{Hz}}$.
- (+) Our noise-tee enables measurements with loss-free source admittances. As a result, the minimum 'cold' level is zero.

Source removal not required

- (–) Distinct hot and cold measurements perform 'cold' measurements with zero reference levels, by replacing the noise source with a loss-free admittance.
- (+) Since our noise-tee is equivalent with a pure transmission line when not in use, there is not necessary to remove it for 'cold' noise measurements. This simplifies the measurement because it saves an additional action.

Generalized extraction algorithm

(-) The distinct hot and cold measurements found in the literature use one hot/cold measurement. They reported a suitable algorithm when the hot/cold measurement has equal source admittance [825,830], and an improved algorithm that corrects for parasitic variation errors when the admittance varies with the effective temperature [831]. This is an inconvenient approach when the method is generalized for several hot and several cold sources, all with different admittances.

(+) The succeeding subsections propose a novel algorithm for extracting noise parameters. They are generalized to facilitate noise extraction for sources, each with an arbitrary effective 'temperature' and admittance.

Minimization of relative errors

(–) State-of-the-art noise extraction algorithms use an over-determined set of equations, and are focused on extracting a plausible solution with minimum error. The algorithms that we found in the literature [823,827,828,832], focus on minimization of *absolute* errors of one or more *noise parameters* (usually the absolute error ΔF).

On the other hand, most applications use these noise parameters to predict the equivalent input noise for a specific source admittance. They require an optimal prediction of *that* value. The accuracy is preferably invariant with the source admittance value, or is optimal for the source admittance of interest. The optimization goal varies with the application. Device modeling applications require usually optimization of the *excesslevel* of the noise current (or voltage), while amplifier applications prefer the optimization of the *hot-level* of the noise current (or voltage).

(+) The algorithms proposed in the succeeding subsection minimize *relative* errors. They minimize the equivalent input excess-noise current. Nevertheless, the train of thought is applicable to a wide range of goal quantities of interest.

The succeeding subsections will demonstrate that our opto-electronic measurement methods, with multi level noise measurements, are capable of full noise-parameter extraction.

8.5.3. Input noise measurements for mismatched source admittances

When designing low noise amplifiers for specific sources then the equivalent noise associated with the specified source admittance is of particularly interest. Measurement of this noise level facilitates the selection of optimal devices and their biasing, having noise-optimal performance for that specific source.

These type of measurements require device noise measurements, in which the source admittance is simulated with an admittance tuner. The two-port noise-tee configuration of section 8.2.4 enables the reproduction of these circumstances with an additional one-port admittance tuner. Figure 8.21 illustrates the basic measurement setup and the various mathematical transformation steps.

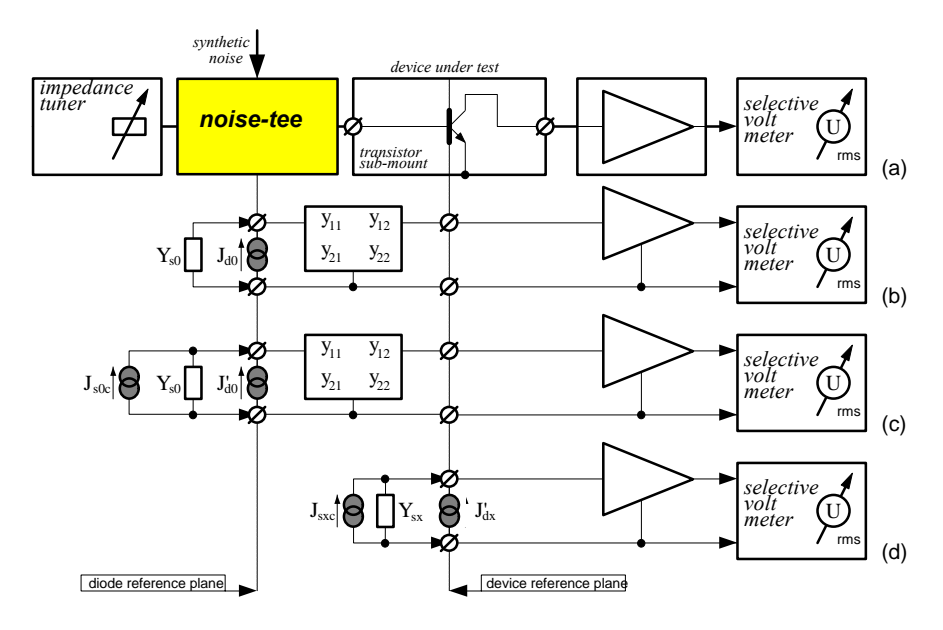


Fig 8.21 Basic measurement setup (a) for the measurement of device noise J_{d0} observed from the diode reference plane for specified admittance Y_{s0} . In (b,c,d) the various steps are illustrated to transform this noise (including thermal noise effects) to the device excess-noise J'_{dx} observed from the device reference plane (excluding thermal noise effects J_{syo}).

Taking it roughly, the measurement and the extraction algorithm consist of the following succeeding steps:

- (1) Measurement of the *hot noise level* J_{d0} of the device noise current, observed from the diode reference plane of the noise-tee, for specified admittance value. An admittance tuner is used to realize this source admittance.
- (2) Extraction of the *excess noise level* J'_{d0} , of the device noise current, by subtracting the *cold noise level* (J_{soc}) due to thermal noise effects in the tuner admittance.
- (3) Transformation of this excess-noise from the diode reference plane to the device reference plane: J'_{dx}

(239)

(4) Addition of thermal noise J_{sxc} when the *hot noise level* of the input noise current is requested, in stead of the excess noise level.

The first step is similar to the ratio measurement on lightwave receivers, as described in section 8.4.4. The other steps are rather similar to the transformation of calibrated noise levels to arbitrary reference planes, as described in the sections 8.3.4 and 8.3.5. The transformation steps and the extraction algorithm for current J'_{dx} are described in detail in appendix L.

To demonstrate the feasibility of our extraction method, the device excess-noise of a bipolar junction transistor are measured for various admittance values. We realized a simple switched admittance tuner with resistors and capacitors, and measured the device excess-noise for six arbitrary settings of the tuner. For a detailed description of this experiment, see Mahmoudi [834].

The device noise was extracted from ratio measurements using four different reference levels. The most plausible device noise was extracted from these values, and then transformed to the device reference plane, using measured two-port parameters and source admittance values. Figure 8.22b shows the extracted device excess-noise current, measured for the source admittance values of figure 8.22a.

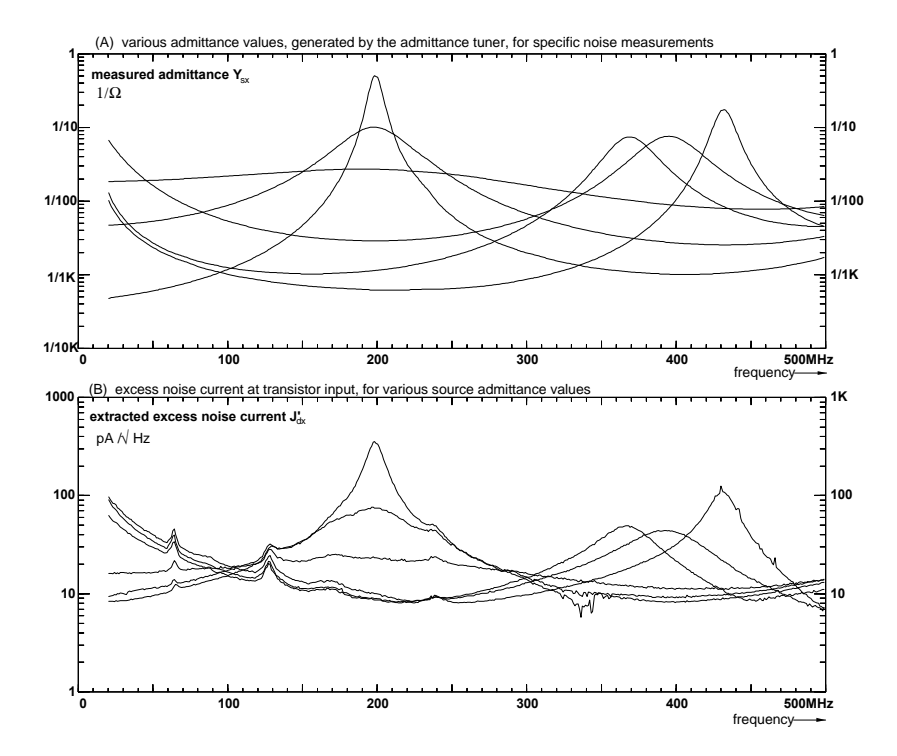


Fig 8.22 Various measured source admittance (a) values Y_{sx} and their associated amplitude spectra (b) of the device excess-noise current J'_{dx} . These measurement are observed from the device reference plane, as illustrated in figure 8.21.

The experimental admittance tuner was composed of resistor-capacitor pairs, shunted to a common 50Ω microstrip transmission line. Manual on and off switching was used to

vary the overall admittance. The tuner, the noise-tee as well as the transistor fixture were constructed from standard epoxy printed circuit boards. The average distance between tuner and device reference plane was approximately 14 cm.

This relative long transmission distance between tuner and DUT has caused the resonant behavior of admittance Y_{sx} . As a result, arbitrary admittance values are restricted to small frequency bands, especially for relatively high and low admittance values (compared to 50Ω). Furthermore this distance has restricted the dynamic range of tuner admittance values for frequencies around 100MHz and 300MHz, observed from the device reference plane. Proper construction will improve the tunability of the source admittance over a wider frequency band.

8.5.4. Extraction of device noise-parameters

This discussion in section 8.5.3 illustrates one can't position the tuner adjustment of a practical setup to *any* admittance of interest. Therefore another approach is required. It requires the prediction of the noise at specified source admittance, based on noise parameter measurements using four or more mis-matched sources. Figure 8.23 illustrates this supplementary approach.

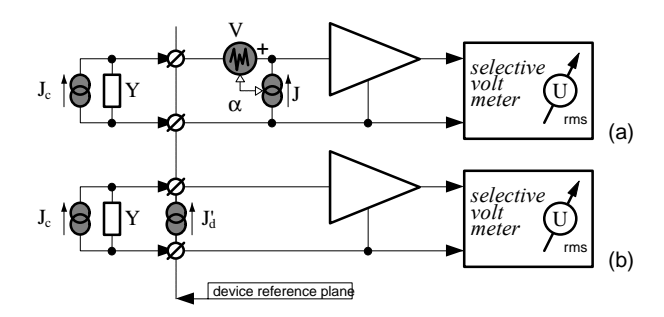


Fig 8.23 The device excess-noise current J_d' for arbitrary source admittance values Y is obtained from a full noise representation of the input port of the device under test. Current J_c is the thermal noise of the source admittance Y ('cold' noise).

Figure 8.23a shows a full noise representation of the device under test, using a correlated pair of a noise voltage source and a noise current source. This model is applicable to any source admittance of interest. Figure 8.23b shows an equivalent representation. Its validation is restricted to the chosen value of the source admittance. The device excess-noise current J'_d is calculated from Y, V, J and their correlation α . Let S_J , and S_V be the (self)-intensity spectra of J(t) and V(t) respectively, let $S_{J|V}$ be their cross-intensity spectrum, and let S_i be the (self) intensity spectrum of the equivalent excess-noise current $J'_d(t)$. As discussed in section 7.3, the following relation holds:

$$\begin{split} S_i &= S_J + |Y|^2 \cdot S_V + 2 \cdot real(Y) \cdot real(S_{J|V}) + 2 \cdot imag(Y) \cdot imag(S_{J|V}) \\ let: & \quad x_1 \stackrel{\text{def}}{=} S_J \\ & \quad x_2 \stackrel{\text{def}}{=} S_V \end{split} \qquad \begin{aligned} x_3 &\stackrel{\text{def}}{=} 2 \cdot re(S_{J|V}) = S_{J|V} + S^*_{J|V} \\ x_4 \stackrel{\text{def}}{=} 2 \cdot im(S_{J|V}) = S_{J|V} - S^*_{J|V} \end{aligned}$$

This is a linear relation, with $[x_1,x_2,x_3,x_4]$ as noise parameters. It illustrates that the overall measurement goal has been focused on the extraction of $[x_1,x_2,x_3,x_4]$, to evaluate the excess-noise intensity S_i .

Note that our primary interest is the prediction of J_d , and not the evaluation of the noise parameters. Therefore, we will restrict our self to a convenient (non-standard) representation format $[x_1,x_2,x_3,x_4]$ to evaluate the device excess-noise for arbitrary source admittances Y. Furthermore, optimal accuracy is required for the excess-noise and not for the noise parameters. Therefore, it is useless to find some optimal solution for $[x_1,x_2,x_3,x_4]$. Instead of that, the extraction algorithm must optimize the relative accuracy of S_i

This work has resulted in two robust extraction algorithms to extract noise parameters from noise measurements. Appendices M and N describe both algorithms in detail.

- The first algorithm, in appendix M, requires information on the input admittance of the device under test. This algorithm is applicable with arbitrary hot and cold measurements. Variation of source impedance is permitted when its noise output level varies. This principle is known from the literature, however the algorithm has been generalized in this study. The algorithm applies for any set of detected noise levels and associated (arbitrary) admittance values.
- The second algorithm, in appendix N does not require any information on the device input impedance. The consequence is that hot and cold measurements are to be performed in pairs with equal source admittance. Another consequence is that more independent levels are to be detected: at least eight (2×4) noise levels instead of five with the previous method. This principle is also known from the literature, however this study has supplemented it with multi level measurements and applied it to sources with noise-tees.

We applied [834] the second algorithm to the extraction of $[x_1,x_2,x_3,x_4]$ from the measurements of figure 8.22. We observed that these noise parameters are applicable for predicting input noise levels for specific source impedances. This is demonstrated in section 8.5.3 for resistive, capacitive and inductive sources.

Additionally, we transformed $[x_1,x_2,x_3,x_4]$ into autonomous noise parameters, as proposed in section 7.3.3, for extracting the parameters of the device noise model discussed in section 7.3.3. We observed that these transformed parameters are quite sensitive to small measurement errors in $[x_1,x_2,x_3,x_4]$. These preliminary results indicate the high demands on measurement accuracy and reproducibility when extracting two-port device models from noise parameter measurements.

8.5.5. Extraction of input noise level for arbitrary source admittances

To demonstrate the feasibility of our second extraction method (see section 8.5.4 and appendix N) with paired (multi-level) hot/cold measurements, the measured [834] results

from figure 8.22 are used to extract the noise parameters of that device. These four parameters are extracted from six independent measurements, each with four reference levels.

From these parameters $[x_1,x_2,x_3,x_4]$, the equivalent excess-noise was predicted for pure capacitive sources, pure inductive sources and pure resistive sources. Figure 8.24 shows the predicted values of the equivalent excess-noise intensity spectrum S_i .

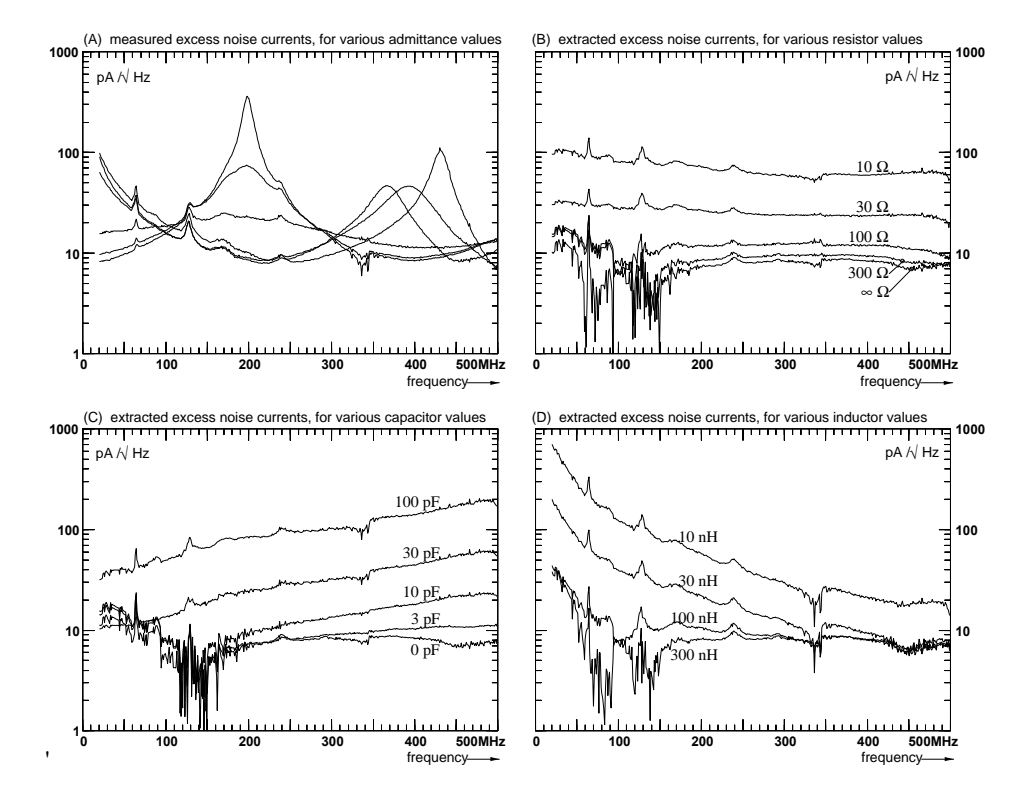


Fig 8.24 Extracted excess-noise current, of a bipolar junction transistor (BFR92a, U_{ce} =10V, I_{c} =10mA, I_{b} =0.25mA), observed at its input. The predictions are based on the extracted noise parameters, using the measurements of figure 8.22.

The excess-noise is the equivalent input noise, minus the thermal noise of the source admittance. It changes with the admittance value.

Figures 8.24b, 8.24c and 8.24d show the reconstructed excess-noise levels S_i , reconstructed for ideal resistive sources, ideal capacitive sources and for ideal inductive sources. They illustrate that the equivalent excess current noise reduces with decreasing admittance. This noise is minimal for infinite admittance values. A significant decrease is not observed above |Z|=300 Ω . These plots are very useful to predict the equivalent input noise for sources with these source impedance values.

Figure 8.24a shows similar plots, associated with admittance values Y that were used for the extraction process (shown in figure 8.22a). As expected, their values match very well with figure 8.22b, which illustrates the validation of our extraction method.

The above examples evaluate the noise parameters as intermediate result. Nevertheless, these parameters can be transformed into any format, e.g. as autonomous noise parameters as discussed in section 7.3.3. This facilitates the development and assessment of adequate transistor noise models.

These noise parameters are extracted, as reported by Mahmoudi [834]. The accuracy, however, of these experimental results is inadequate to perform reliable model extraction. The spikes and dips in the extracted values, shown in figure 8.24, are indicative for the high accuracy and reproducibility that is required for these types of measurements. As a result, improvements of the measurement are aspects for further investigations.

8.5.6. Conclusions

In conclusion, various state-of-the-art methods are summarized to measure the input noise parameters of a device under test. The difference between the methods is characterized by the need for two-port measurements, the need for one-port measurement or no transfer measurement at all.

Several improvements are discussed that may result when applying our noise-tee to state-of-the-art methods.

It has been demonstrated that our opto-electronic measurement methods, with multi level noise measurements, are capable of full noise parameter extraction. Novel algorithms are developed for extracting noise parameters. They are generalized to facilitate noise extraction for sources, each with an arbitrary effective 'temperature' and admittance.